Check for updates

Interferon-gamma ameliorates experimental autoimmune encephalomyelitis by inducing homeostatic adaptation of microglia

Juan E. Tichauer[1†], Gabriel Arellano[1,2†], Eric Acuña[1],
Luis F. González[1], Nirmal R. Kannaiyan[3], Paola Murgas[4],
Concepción Panadero-Medianero[4], Jorge Ibañez-Vega[1],
Paula I. Burgos[5], Eileah Loda[2], Stephen D. Miller[2],
Moritz J. Rossner[3], Peter J. Gebicke-Haerter[1,6]
and Rodrigo Naves[1*]

[1]Program of Immunology, Institute of Biomedical Sciences, Faculty of Medicine, Universidad de Chile,
Santiago, Chile, [2]Department of Microbiology-Immunology, Feinberg School of Medicine,
Northwestern University, Chicago, IL, United States, [3]Molecular Neurobiology, Department of
Psychiatry & Psychotherapy, Ludwig-Maximilians-University of Munich, Munich, Germany, [4]Center for
Integrative Biology, Faculty of Science, Universidad Mayor, Santiago, Chile, [5]Department of Clinical
Immunology and Rheumatology , School of Medicine, Pontificia Universidad Católica de Chile,
Santiago, Chile, [6]Central Institute of Mental Health, Faculty of Medicine, University of Heidelberg,
Mannheim, Germany

Compelling evidence has shown that interferon (IFN)-γ has dual effects in multiple sclerosis and in its animal model of experimental autoimmune encephalomyelitis (EAE), with results supporting both a pathogenic and beneficial function. However, the mechanisms whereby IFN-γ may promote neuroprotection in EAE and its effects on central nervous system (CNS)-resident cells have remained an enigma for more than 30 years. In this study, the impact of IFN-γ at the peak of EAE, its effects on CNS infiltrating myeloid cells (MC) and microglia (MG), and the underlying cellular and molecular mechanisms were investigated. IFN-γ administration resulted in disease amelioration and attenuation of neuroinflammation associated with significantly lower frequencies of CNS CD11b$^+$ myeloid cells and less infiltration of inflammatory cells and demyelination. A significant reduction in activated MG and enhanced resting MG was determined by flow cytometry and immunohistrochemistry. Primary MC/MG cultures obtained from the spinal cord of IFN-γ-treated EAE mice that were *ex vivo* re-stimulated with a low dose (1 ng/ml) of IFN-γ and neuroantigen, promoted a significantly higher induction of CD4$^+$ regulatory T (Treg) cells associated with increased transforming growth factor (TGF)-β secretion. Additionally, IFN-γ-treated primary MC/MG cultures produced significantly lower nitrite in response to LPS challenge than control MC/MG. IFN-γ-treated EAE mice had a significantly higher frequency of CX3CR1^{high} MC/MG and expressed lower levels of program death ligand 1 (PD-L1) than PBS-treated mice. Most CX3CR1^{high}PD-L1^{low}CD11b$^+$Ly6G$^-$ cells expressed MG

markers (Tmem119, Sall2, and P2ry12), indicating that they represented an enriched MG subset (CX3CR1highPD-L1low MG). Amelioration of clinical symptoms and induction of CX3CR1highPD-L1low MG by IFN-γ were dependent on STAT-1. RNA-seq analyses revealed that *in vivo* treatment with IFN-γ promoted the induction of homeostatic CX3CR1highPD-L1low MG, upregulating the expression of genes associated with tolerogenic and anti-inflammatory roles and down-regulating pro-inflammatory genes. These analyses highlight the master role that IFN-γ plays in regulating microglial activity and provide new insights into the cellular and molecular mechanisms involved in the therapeutic activity of IFN-γ in EAE.

1 Introduction

Multiple Sclerosis (MS) is a disease of the central nervous system (CNS) characterized by chronic inflammation and demyelination. It is the most common autoimmune disease in the brain and the leading cause of non-traumatic neurological disability in young adults (1). Experimental autoimmune encephalomyelitis (EAE) remains the animal model most widely used to study disease mechanisms and therapeutic approaches for MS (2). EAE is actively induced by immunization with myelin-derived antigens associated with adjuvant and consists of an induction phase and an effector phase (3). The induction phase involves the priming of myelin epitope-specific CD4+ T cells in the periphery. The effector phase is characterized by innate and adaptive immune cell migration from the periphery into the CNS and their re-activation by CNS resident cells such as microglia (MG) or immigrating antigen-presenting cells (APC) (2, 3). Both MS and EAE are characterized by inflammatory lesions in the CNS that mainly contain cells expressing the CD11b cell marker (4). This CD11b+ cell population includes peripheral myeloid cells (MC) such as neutrophils, monocytes, dendritic cells, and macrophages as well as CNS resident MG.

MG constitute about 5-20% of all cells in the CNS (5) and their primary role is the support and maintenance of CNS as well as to perform important surveillance functions (6). MG are characterized by a prominent expression of the fractalkine receptor CX3CR1, which is not expressed in astrocytes, oligodendrocytes, or neurons (7, 8). Indeed, CX3CR1 promotor activity has been used for the visualization, genetic manipulation, and the study of the function of MG in the CNS (9). In addition, CX3CR1 is considered a microglial homeostatic marker (10, 11) and lack of this receptor results in exacerbation of inflammation and increased expression of MHC class II molecules in MG (12–14). During early stages of demyelination, active lesions present increased numbers of MG expressing pro-inflammatory markers associated with phagocytosis, antigen presentation and T cell co-stimulation. In later stages, MG develop an intermediate phenotype between pro- and anti-

inflammatory activation. Interestingly, loss of homeostatic microglial signature observed in active lesions of MS patients is restored during disease inactivity (15, 16). Therefore, MG have the capability of producing a wide variety of molecules that allow them to exert both inflammatory/detrimental and anti-inflammatory/protective functions in EAE and MS (16).

Interferon gamma (IFN-γ), the only member of the type II IFN family, is a cytokine that has been historically considered the hallmark of Th1 cells driving inflammation in EAE and MS (17, 18). However, compelling evidence has challenged the notion that IFN-γ is strictly pathogenic and has been ascribed a protective role as well [reviewed in (19–21)]. Several studies analyzing EAE development in mice either deficient in the IFN-γ gene, lacking the IFN-γ receptor, or treated with neutralizing antibodies against IFN-γ, demonstrate that endogenous IFN-γ plays a disease-limiting role in EAE (22–33). Likewise, EAE symptoms are ameliorated in response to IFN-γ administered systemically (i.p.) (29, 30) or directly into the CNS (33). Therefore, IFN-γ has opposite effects in EAE, which can be explained, at least in part, through its dose-dependent dual action on MG. Low doses of IFN-γ enable MG to perform neuroprotective functions, whereas high doses of IFN-γ polarize MG toward an inflammatory state [reviewed in (20)]. In EAE, we and other investigators have found that IFN-γ is detrimental during the induction phase but protective during the early effector phase (acute phase) (26, 32, 34, 35), indicating that opposing effects of IFN-γ depend on the stage of the disease. However, the mechanisms whereby IFN-γ is able to exert protection in EAE and its role at the peak of EAE remain unresolved. Moreover, most studies concerning the role of IFN-γ in the pathogenesis and progression of EAE and MS have primarily focused on peripheral lymphoid cells while its action on CNS-infiltrating myeloid cells and CNS-resident cells such as MG has been largely ignored, despite their critical role in regulating autoimmune neuroinflammation. This study aims to elucidate the impact of systemic administration of IFN-γ at the peak of EAE, its effects on CNS infiltrating MC and MG, and the underlying cellular and molecular mechanisms.

2 Material and methods

2.1 Mice

C57BL/6 mice and the Signal Transducer and Activation Transcription (Stat)-1$^{-/-}$ (B6.129S(Cg)-Stat1tm1Dlv/J, stock #012606) mice were obtained from The Jackson Laboratory. C57BL/6J MOG$_{35-55}$-specific TCR transgenic (2D2) mouse strain was kindly provided by Dr. R Pacheco (Fundación Ciencia & Vida, Chile). All mice were maintained under specific pathogen-free (SPF) conditions. All experimental procedures complied with the Helsinki Declaration of animal experiments and were approved by the Institutional Animal Care and Use Committee (IACUC) of the University of Chile and Northwestern University.

2.2 Induction of EAE and treatment

EAE was induced in 8- to 12-week-old mice with a s.c. injection of 150 µg myelin oligodendrocyte glycoprotein-derived 35-55 peptide (MOG$_{35-55}$, MEVGWYRSPFSRVVHLYRNGK, CPC Scientific, California, US), emulsified in Incomplete Freund's adjuvant containing 500 µg *Mycobacterium tuberculosis* (BD Difco, Detroit, Michigan, US) followed by an i.p. injection with 500 ng *Bordetella pertussis* toxin (List Biological, Campbell, California, US) on the day of immunization and 48 h later. Body weight and clinical symptoms were monitored daily using a standard clinical score of 0-6 as previously described (36). For treatment with IFN-γ, 1 µg/mouse/day of recombinant murine IFN-γ (Biolegend, San Diego, California, US) was administered i.p. for 5 days starting at the peak of EAE. Non-immunized (NI) mice (without EAE) and EAE mice injected with phosphate-buffered saline (PBS) (Gibco, Grand Island, New York, US) were used as control groups (Figure 1A).

2.3 Histological analysis

Mice were deeply anesthetized and intracardially perfused with PBS (0.1 M) followed by 4% paraformaldehyde (pH=7.4). Thoracic and lumbar spinal cord (SC) sections were removed, post-fixed in 4% paraformaldehyde, and embedded in paraffin. Serial sections with 6 µm thickness were cut, followed by hematoxylin and eosin (H&E) and luxol fast blue (LFB) staining. All reagents were purchased from Sigma (Saint Louis, Missouri, USA). LFB images were captured on an Olympus BX51 multichannel light/epifluorescence microscope (Olympus, Tokyo, Japan). H&E images were captured on a NanoZoomer XR slide scanner (Hamamatsu Photonics, Japan) employing the NanoZoomer Digital Pathology scan software v3.0 (Hamamatsu Photonics,
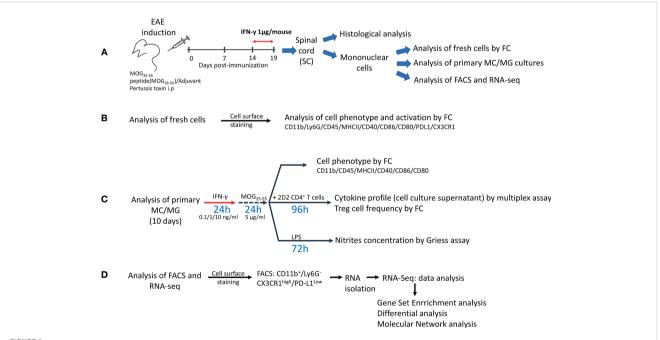

FIGURE 1

Experimental design. **(A)** Mice were immunized with myelin oligodendrocyte protein peptide (MOG$_{35-55}$) to induce experimental autoimmune encephalomyelitis (EAE). Mice were treated daily with 1 µg/mouse of mrIFN-γ or PBS for 5 days at the peak of EAE. SC were collected for histological analysis or to isolate mononuclear cells, which were used for analysis of fresh cells by multiparametric flow cytometry (FC), primary myeloid cells/microglia (MC/MG) cultures, fluorescence activated cell sorting (FACS), and RNAseq analysis. **(B)** Fresh isolated cells were used to determine the cell phenotype by FC analysis using the markers described in the figure. **(C)** Primary MC/MG cultures were established and then cells were pre-conditioned with low doses of IFN-γ (0.1, 1, and 10 ng/ml) for 24 h and then pulsed with MOG$_{35-55}$ (5 µg/ml) for an additional 24 h. Cells were analyzed for tolerogenic phenotype by FC or were co-cultured with 1x10^6 CD4$^+$ T cells obtained by negative selection from spleens of 2D2 mice. After 4 days of co-culture, supernatants were collected for further cytokine analysis by multiplex assay or ELISA and the cells were analyzed for Treg cell frequency (CD4$^+$CD25^{high}Foxp3$^+$) by FC. In other assays, pre-conditioned MC/MG cultures were challenged with 1 µg/ml LPS for 72 h. Cell culture supernatant was collected and nitrite was determined by Griess reaction. **(D)** Fresh isolated cells were stained with antibodies against CD11b, LY6G, CD45, CX3CR1 and PD-L1, and immediately sorted on a FACSAria^{TM} III. RNA was isolated using RNAeasy Micro kit and used for RNAseq analysis.

Japan). Density of infiltrating inflammatory cells was determined as the number of cell nuclei per 10.000 μm^2. The extent of demyelination was evaluated by measuring the percentage of demyelinated area over the total white matter area for each SC section. Quantifications were performed using ImageJ software (NIH, USA).

2.4 Immunohistochemistry

For immunostaining, thoracic SC sections were deparaffinized and rehydrated. Heat-induced antigen retrieval was performed in citrate buffer (pH=6.0) for 30 min. Sections were washed in 1X Tris-buffered saline (TBS), permeabilized, and blocked for 1 h at room temperature (RT) in blocking buffer [5% bovine serum albumin (BSA), 0.5% Triton-X 100 in 1X TBS)]. Tissues were incubated with the primary antibody polyclonal rabbit anti-ionized-calcium binding adaptor protein (Iba) 1 diluted in blocking buffer (1:300, FujiFilm Wako, Osaka, Japan) overnight at 4°C. The next day, slides were washed with 1X TBS and incubated with Alexa Fluor

555-labeled secondary antibody anti-rabbit (1:200, Invitrogen, Waltham, MA, US) for 3 h at RT (Table 1). Slides were washed with 1X TBS, and cell nuclei were stained with 4',6-diamidino-2-phenylindole (DAPI). Finally, slides were rinsed with 1X TBS, mounted with an anti-fade mounting media, and visualized in a Leica DMI8 inverted fluorescence microscope. Image J-assisted analysis was used to evaluate density of Iba1^{+} cells, determined as the number of Iba1^{+} cells per 100.000 μm^2; average Iba1^{+} cell size, determined as cell area of Iba1^{+} cells; and percentage Iba1 coverage, determined as the percentage of the total section area occupied by Iba1^{+} cells (μm^2).

2.5 Cell cultures and ex vivo re-stimulation

Mononuclear cells were isolated from SC of EAE mice treated with PBS or IFN-γ at day 19 post-immunization as previously described (37). Briefly, spinal cord homogenates were obtained and incubated with 0.5 mg/ml collagenase (Roche, Manheim, Germany) and 10 units/ml DNAse I (New England Biolabs, Ipswich,

TABLE 1 List of antibodies used for immunofluorescence and flow cytometry.

Specificity	Fluorochrome	Dilution	Source	Clone/ID
Neutrophil				
LY6G	BV605	1:500	BIOLEGEND	1A8
Microglia				
TMEM119	Unconjugated (Rabbit)	1:100	ABCAM	106-6
	anti-rabbit Alexa fluor 555	1:1000	INVITROGEN	AB_2535849
Myeloid cells/Microglia				
Iba1	Unconjugated (Rabbit)	1:300	WACO	Polyclonal
	anti-rabbit Alexa fluor 555	1:200	INVITROGEN	AB_2535849
CD11b	FITC/PE	1:300	BIOLEGEND	M1/70
CD45	APC	1:500	BIOLEGEND	30-F11
CX3CR1	PE/Cy7	1:500	BIOLEGEND	SA011F11
PD-L1 (CD274; B7-H1)	BV711	1:400	BIOLEGEND	10F.9G2
MHCII	Alexa Fluor700	1:600	EBIOSCIENCE	MS/114.15.2
CD86	APC/Cy7	1:400	BIOLEGEND	GL-1
CD80	PE	1:200	BIOLEGEND	16-10A1
CD40	PerCP	1:300	BIOLEGEND	3/23
CD4^{+} Treg cells				
CD4	FITC	1:200	BIOLEGEND	RM4-5
CD25	APC	1:200	BIOLEGEND	PC61
FoxP3	PE	1:200	BIOLEGEND	150D
Myelin				
MBP1	Unconjugated (Mouse)	1:70	BIOLEGEND	SMI99
	anti-mouse Alexa fluor 555	1:500	INVITROGEN	AB_2535844

APC, allophycocyanin; BV,brilliant violet; Cy, cyanine; FITC, fluorescein isothiocyanate; PE, phycoerythrin; PERCP, Peridinin Chlorophyll Protein Complex.

Massachusetts, US) at 37°C for 1 h. Mononuclear cells were purified using 40%/70% discontinuous Percoll gradients (Amersham, Piscataway, New Jersey, US), and total cell numbers were determined using a hemocytometer with viability assessed by trypan blue exclusion. In some assays, fresh cells were immediately analyzed by flow cytometry (Figure 1B). In other experiments, primary cell cultures were established; seeding cells in 24-well plates at a density of $2x10^5$ cells per well in 1 ml Iscove´s Modified Dulbecco´s Medium (IMDM) supplemented with 10% fetal calf serum (FCS), 100U/ml penicillin plus 100 µg/ml streptomycin, 1 mM sodium pyruvate, 50 µM beta-mercaptoethanol, 2 mM glutamine, and non-essential amino acids (all from Gibco, Carlsbad, California, US) (Figure 1C). Primary cell cultures usually contained 80-90% of adherent CD11b$^+$ myeloid/microglia (MC/MG) (Supplementary Figure 1). For nitric oxide (NO) determination, MC/MG were re-stimulated with 1 ng/ml IFN-γ for 24 h and then pulsed with 5 µg/ml MOG$_{35-55}$ for an additional 24 h. Then, re-stimulated MC/MG cultures were challenged with 1 µg/ml bacterial lipopolysaccharide (LPS) for 72 h in IMDM culture media. Thereafter, the medium was collected, and nitrite, a stoichiometric and stable metabolite of NO, was determined from supernatants by Griess reaction (Promega, Madison, Wisconsin, US). For cell co-culture experiments, MC/MG were re-stimulated with varying amounts of IFN-γ (0.1-1-10 ng/ml) for 24 h, washed, and then pulsed with MOG$_{35-55}$ (5 µg/ml) for an additional 24 h. After washing, cells were co-cultured with $1x10^6$ CD4$^+$ T cells previously purified by negative selection from spleens of 2D2 mice using a CD4$^+$ T cell isolation kit (Miltenyi Biotec, Bergisch Gladbach, Germany). After 4 days of co-culture, cell culture supernatant was collected for further cytokine analysis, and the cells were analyzed for Treg cell frequency (CD4$^+$CD25^{high}Foxp3$^+$) by flow cytometry (Figure 1C).

2.6 Immune staining, flow cytometry, and FACS Sorting.

For cell surface staining, isolated cells were immediately fixed with fixation buffer (eBioscience, San Diego California, US) overnight at 4°C. For blocking non-specific Fc receptor-mediated antibody binding, cells were incubated with anti-FcγR III/II antibody for 15 min at 4°C in 2% fetal calf serum (FCS) PBS. Then, cells were stained with antibodies against CD11b, lymphocyte antigen 6 complex locus G (LY6G), CD45, CX3C chemokine Receptor 1 (CX3CR1), programmed death ligand 1 (PD-L1), CD86, CD80, CD40, MHC class II (MHC-II) molecules, and transmembrane protein (TMEM) 119 for 30 minutes at 4°C (Table 1). For intracellular staining, cells were permeabilized with Permeabilization kit (eBioscience, San Diego California, US) for 30 minutes at RT and then incubated with antibodies against forkhead box P3 (FoxP3) (Biolegend, USA) for 30 minutes at RT. Next, cells were resuspended in PBS and analyzed using a Fortessa Flow Cytometer (BD Biosciences, USA) and FlowJo software (Tree Star, USA). Flow cytometry gating strategies are described in Supplementary Figure 2.

For FACS (Figure 1D), freshly isolated SC cells of 5-6 mice were incubated with anti-FcγR III/II antibody for 15 min at 4°C in 2% FCS PBS and immune stained with antibodies against CD11b, LY6G, CD45, CX3CR1, PD-L1, for 30 minutes at 4°C. Cells were immediately sorted on a FACSAria^{TM} III (BD Biosciences, US), collected in tubes containing 2.4 ml of RLT lysis buffer (Qiagen, Hilden, Germany), and frozen at -80°C until RNA-Seq analysis. Usually, $6x10^4$ to $1x10^5$ cells were obtained, and cell viability was higher than 97% (not shown). Post sorting analysis confirmed that >97.5% of sorted cells were CD11b$^+$LY6G$^-$CX3CR1^{high}PD-L1^{low}.

2.7 Cytokine analysis

The concentration of IFN-γ, IL-1β, tumor necrosis factor (TNF)-α, granulocyte macrophage colony-stimulating factor (GM-CSF), IL-2, IL-4, and IL-10 in cell co-culture supernatants was determined by a multiplex assay using Luminex technology (Merck Millipore, Darmstadt, Germany) according to manufacturer´s instructions. Total and active transforming growth factor (TGF)-β production was determined by ELISA (Invitrogen, Vienna, Austria). The standard curve was diluted in medium containing 10% fetal calf serum, so TGF-β production was calculated over the basal level contained in the fetal calf serum (Figure 1C).

2.8 RNA sequencing analysis

2.8.1 Library preparation and sequencing

RNA was isolated from CD11b$^+$Ly6G$^-$CX3CR1^{high}PD-L1^{low}cells obtained from SC of EAE mice treated with either IFN-γ or PBS using RNAeasy Micro kit (Qiagen, Hilden, Germany) (Figure 1D). 1 µl of ERCC RNA Spike-In Mix (ThermoFisher, Carlsbad, California, US) diluted 1:5000 was added to the isolated RNA as an external control. cDNA was synthesized using Ovation RNA-Seq System V2 (NuGen, Groningen, Netherlands). 100 ng of cDNA was used as input for fragmentation and followed by library preparation using the IonXpress plus gDNA and Amplicon Library preparation kit (ThermoFisher, Carlsbad, California, US) as described by the manufacturer. The library was then size selected on a 2% E-Gel (ThermoFisher, Carlsbad, California, US). Sample specific barcodes were then added and amplified. Individual sample libraries were quantified using a Kapa Library Quantification Kit (Kapa, Wilmington, Massachusetts, US) using samples diluted 1:200. Equal quantities of individual samples were then pooled and sequenced on an Ion Proton Sequencer.

2.8.2 Data analysis

The raw reads (Fastq) were split into sample-specific reads based on the barcodes. The reads were then checked for sequence quality and sequence repeats. Low-quality bases and short reads were removed from further analysis. The reads were subsequently mapped to the Mus musculus genome (mm10) using TMAP Aligner and quantified using Ensembl annotation 86 using Partek Flow. Genes with a minimum of 5 reads in at least 80% of the samples were considered for further analysis. Differentially expressed genes (DEGs) were determined in R with the DESeq2 package (38). Genes with at least one-fold change and corrected p-Value of less than 0.05 were considered as differentially expressed between IFN-γ-treated and PBS control mice. Gene set enrichment

analysis (GSEA) was performed using the gene sets from the Molecular Signatures Database-MsigDB. Overrepresentation analysis was performed using Reactome database (a database of reactions, pathways, and biological processes) (39, 40).

2.8.3 Construction of a molecular network of protein interactions

In order to search for molecular connections between selected genes, each gene was subjected to a nearest neighbor or cluster analysis using the STRING platform (https://string-db.org/). The setting of 100 interactions (custom value) and a minimum score of 0.400 (medium confidence) was chosen. The lists for each gene were entered into "genes.R " available in "R" (https://cran.r-project.org/bin/windows/base/) and turned into a graphical display by using "igraph", a network analysis R package (http://igraph.org/r/).

2.9 Statistical analysis

Results were analyzed using a Mann–Whitney nonparametric test or one-way ANOVA using GraphPad Prism v.5.0 (GraphPad Software). P values <0.05 were considered statistically significant.

3 Results

3.1 IFN-γ treatment induces amelioration of the clinical symptoms and attenuation of neuroinflammation at the peak of EAE

First, we determined the effect of systemic administration of IFN-γ for 5 days starting at the peak of EAE. The results showed that IFN-γ significantly decreased the severity of clinical symptoms and body weight loss compared to PBS-treated mice (Figure 2A). After cessation of treatment, disease severity returned to levels similar to PBS-treated mice (Supplementary Figure 3). Histological analyses showed that thoracic and lumbar SC sections from IFN-γ-treated EAE mice had significantly less infiltration of inflammatory cells and fewer demyelinated areas compared to PBS-treated-EAE mice (Figures 2B, C). Interestingly, flow cytometry analysis revealed that *in vivo* IFN-γ-treatment resulted in a significantly lower absolute number of mononuclear cells and lower frequency and absolute numbers of CD11b$^+$ cells and non-neutrophil MC/MG (CD11b$^+$Ly6G$^-$) compared to SC from PBS-treated EAE mice; however, levels were still higher than the non-immunized (NI) group (Figure 3A–C). There was no significant difference in the frequency and absolute number of neutrophils (CD11b$^+$Ly6G$^+$) between the PBS- and IFN-γ-treated mice (Figure 3D). Similar total number of cells was determined in draining lymph nodes (dLN) and spleen from IFN-γ-treated EAE mice and control mice. Frequency and absolute number of CD11b$^+$ cells and neutrophils and macrophages in dLN was not affected by IFN-γ treatment. In contrast, a significantly lower frequency and absolute number of CD11b$^+$ cells and neutrophils were found in spleen from IFN-γ-treated EAE mice compared to those from PBS-treated EAE mice; whilst macrophages were not significantly altered (Supplementary Figure 4).
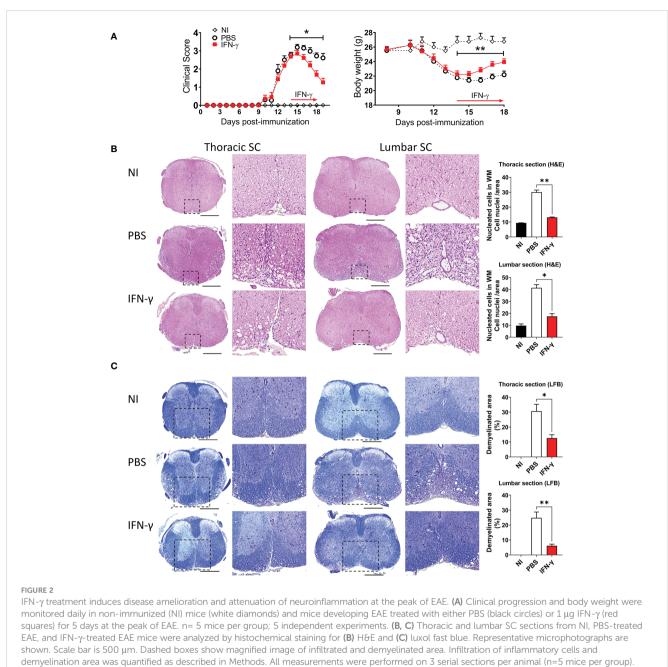
Several studies have reported that in a neuroinflammatory or tumor microenvironment MG are induced to upregulate CD45 expression (5, 41–49). Consequently, an increase in the frequency of CD45^{hi} cells would reflect the activation of CD45^{low} MG into CD45^{hi} cells resembling peripheral infiltrating MC (44–46). Our results showed that IFN-γ-treatment resulted in a significantly lower frequency and absolute number of activated MC/MG cells (CD11b$^+$Ly6G$^-$CD45^{high}) compared to PBS-treatment. In addition, IFN-γ-treatment induced a significant increase in the percentage of resting MG compared to PBS-treated EAE mice; but was still lower than NI mice (Figure 3E, F). Consistent with the activation status of these cell populations, activated MC/MG (CD11b$^+$Ly6G$^-$CD45^{high}) obtained from both IFN-γ- and PBS-treated EAE mice showed a significantly higher expression of MHC-II molecules, CD80, CD40, and PD-L1 than resting MG (CD11b$^+$Ly6G$^-$CD45^{low}) (Supplementary Figure 5).

Resting MG are also characterized by a ramified cell morphology with numerous thin processes that upon activation are drawn back into the soma, resulting in a rounded amoeboid-like appearance. In order to evaluate morphological changes associated with microglial activation, thoracic SC sections from NI mice and IFN-γ- and PBS-treated EAE mice were immunostained for Iba1, a known cell marker used to evaluate MC/MG morphology and activation (50–54). SC from PBS-treated mice were characterized by extensive Iba1 staining and amoeboid-shaped Iba1$^+$ cells. Instead, IFN-γ-treated mice had predominantly ramified-shaped, Iba1-stained cells similar to NI mice (Figure 4A). In addition, SC from IFN-γ-treated EAE mice showed the density of Iba1$^+$ cells, average Iba1$^+$ cell area (indicative of cell size), and percentage Iba1 coverage (indicative of simultaneous alterations in cell density and morphology) significantly reduced in comparison to PBS-treated mice, but similar to NI mice (Figure 4B–D).

IFN-γ also plays a protective role in preventing hindbrain neuroinflammation, an effect dependent on the interaction between IFN-γ and CNS cells (55–57). Therefore, changes in MG and myelination in the cerebellum obtained from EAE mice treated with IFN-γ or PBS by immunofluorescence were examined. A significantly higher expression of TMEM119, a recently described homeostatic marker for MG (11, 58), and of MBP staining was observed in response to IFN-γ compared to control treatment (Supplementary Figure 6; Method S1). Taken together, these results indicate that *in vivo* IFN-γ-treatment starting at the peak of EAE induces amelioration of clinical symptoms, reduction of body weight loss, attenuation of neuroinflammation associated with significantly less infiltration of inflammatory cells and demyelination, reduced activation of MC/MG, and enhanced expression of homeostatic microglial markers.

3.2 Ex vivo re-stimulation with low doses of IFN-γ and MOG$_{35-55}$ induces tolerogenic and anti-inflammatory activity in MC/MG from IFN-γ-treated EAE mice

It has been reported that low concentrations of IFN-γ induce a tolerogenic phenotype in MG from neonatal mice capable of inducing regulatory T (Treg) cells (59). Thus, we were interested in determining the tolerogenic activity and phenotype of primary MC/MG cultures established from EAE-induced mice treated with

FIGURE 2

IFN-γ treatment induces disease amelioration and attenuation of neuroinflammation at the peak of EAE. **(A)** Clinical progression and body weight were monitored daily in non-immunized (NI) mice (white diamonds) and mice developing EAE treated with either PBS (black circles) or 1 μg IFN-γ (red squares) for 5 days at the peak of EAE. n= 5 mice per group; 5 independent experiments. **(B, C)** Thoracic and lumbar SC sections from NI, PBS-treated EAE, and IFN-γ-treated EAE mice were analyzed by histochemical staining for **(B)** H&E and **(C)** luxol fast blue. Representative microphotographs are shown. Scale bar is 500 μm. Dashed boxes show magnified image of infiltrated and demyelinated area. Infiltration of inflammatory cells and demyelination area was quantified as described in Methods. All measurements were performed on 3 serial sections per animal (n=5 mice per group). Results are shown as the mean ± SEM. *P <0.05; **P <0.01.

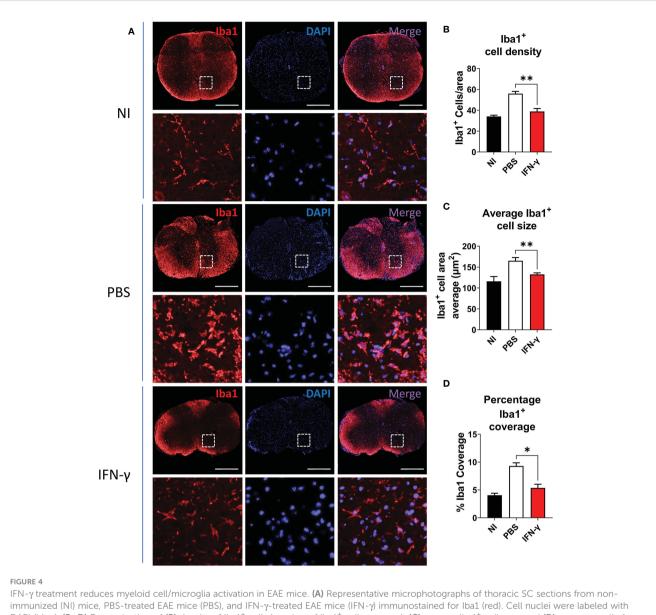IFN-γ or PBS. First, cell cultures were *ex vivo* pre-conditioned with low doses (0.1, 1, and 10 ng/ml) of IFN-γ and MOG$_{35-55}$, and then co-cultured with CD4$^+$ T cells obtained from transgenic 2D2 mice for 96 h (Figure 1C). The results showed that MC/MG obtained from IFN-γ-treated EAE mice and *ex vivo* stimulated with 0.1 and 1 ng/ml IFN-γ induced a significantly higher frequency of Treg cells compared to untreated cells. Interestingly, *ex vivo* re-stimulation with 1 ng/ml IFN-γ and MOG$_{35-55}$ induced a significantly higher frequency and absolute number of Treg cells in co-cultures containing MC/MG obtained from IFN-γ-treated EAE mice than in co-cultures containing MC/MG from PBS-treated EAE mice (Figure 5A). No differences in the expression of MHC-II, CD86, CD80, and CD40 in primary MC/MG obtained from either IFN-γ-

treated EAE mice or PBS-treated mice and stimulated with low doses of IFN-γ and MOG$_{35-55}$ were detected prior to culture with 2D2 CD4$^+$ T cells (Figure 5B). Cell culture supernatants obtained at the end of the co-cultures of pre-conditioned MC/MG and 2D2 CD4$^+$ T cells were analyzed by immunoassays. Cell co-cultures containing MC/MG obtained from IFN-γ-treated EAE mice had lower production of IFN-γ, TNF-α, and GM-CSF than conditioned cell co-cultures containing MC/MG obtained from PBS-treated EAE mice. However, only the secretion of IFN-γ in co-cultures containing MC/MG from IFN-γ-treated EAE mice and pre-conditioned with 10 ng/ml IFN-γ and MOG$_{35-55}$ was statistically lower than in those from control mice. Interestingly, cell co-cultures containing MC/MG isolated from IFN-γ-treated EAE mice and *ex*

FIGURE 3

IFN-γ treatment induces a decrease in the number of spinal cord mononuclear cells, a reduction of activated myeloid cell/microglia, and an increase of resting microglia. SC from non-immunized (NI) mice (black bar) and mice developing EAE treated with either PBS (white bar) or 1 μg IFN-γ (red bar) were used to determine **(A)** number of mononuclear cells. **(B-D)** Frequency (top panel) and absolute cell number (bottom panel) of **(B)** CD11b$^+$ cells, **(C)** myeloid cell/microglia (MC/MG) (CD11b$^+$Ly6G$^-$), and **(D)** neutrophils (CD11b$^+$Ly6G$^+$) were determined by flow cytometry. **(E)** Flow cytometry gating for the determination of activated MC/MG (CD11b$^+$Ly6G$^-$CD45^{high}) and resting MG (CD11b$^+$Ly6G$^-$CD45^{low}). **(F)** Frequency and absolute cell number of activated MC/MG and resting MG were determined by flow cytometry. Values In flow cytometry plots indicate the percentage of positive cells in each gate or quadrant. n= 5 mice per group; 5 independent experiments. Results are shown as the mean ± SEM. *P <0.05; **P <0.01.

vivo pre-conditioned with 1 ng/ml IFN-γ and MOG$_{35-55}$ showed a significantly higher production of total TGF-β than control co-cultures (Figure 5C). Furthermore, active TGF-β production was higher in co-cultures containing MC/MG isolated from IFN-γ-treated EAE mice and *ex vivo* conditioned with 1 and 10 ng/ml IFN-γ and MOG$_{35-55}$ than control co-cultures (Figure 5C). In contrast, cell co-cultures containing MC/MG obtained from PBS-treated EAE mice and stimulated *ex vivo* with low doses of MOG$_{35-55}$ alone or in combination with IFN-γ produced significantly lower levels of active TGF-β than unstimulated cell co-cultures. There was

no difference in the production of IL-4, IL-10, IL-2, and IL-1β between both groups of co-cultures. These results suggest that *ex vivo* re-stimulation with low doses of IFN-γ and MOG$_{35-55}$ endow MC/MG with the capacity to induce conversion of CD4$^+$ T cells into Treg cells in association with high secretion of TGF-β.

Since nitric oxide (NO) is recognized as an important effector molecule produced by macrophages and microglia in response to inflammation (60), we evaluated NO production. Pre-conditioned MC/MG cultures obtained from IFN-γ-treated EAE mice produced significantly lower nitrite in response to LPS stimulation than those

FIGURE 4

IFN-γ treatment reduces myeloid cell/microglia activation in EAE mice. **(A)** Representative microphotographs of thoracic SC sections from non-immunized (NI) mice, PBS-treated EAE mice (PBS), and IFN-γ-treated EAE mice (IFN-γ) immunostained for Iba1 (red). Cell nuclei were labeled with DAPI (blue). **(B–D)** Determination of **(B)** density of Iba1$^+$ cells (number of Iba1$^+$ cells per area), **(C)** average Iba1$^+$ cell area, and **(D)** percentage Iba1 coverage (percentage of the total section area occupied by Iba1$^+$ cells). All measurements were performed on 3 serial sections per animal (n=5 mice per group). Scale bar is 500 μm. Results are shown as the mean $\pm$ SEM. *P <0.05; **P <0.01.

from PBS-treated EAE mice (Figure 5D). Taken together, these results show that *ex vivo* re-stimulation with low doses of IFN-γ and MOG$_{35-55}$ induces tolerogenic and anti-inflammatory activity in MC/MG.

3.3 In vivo IFN-γ-treatment induces increased frequency of CX3CR1^{high}PD-L1^{low} MG in a STAT-1-dependent manner

Next, we examined the expression of MHC class II molecules, costimulatory molecules (CD80, CD86, CD40), coinhibitory molecules (PD-L1), and a microglial marker (CX3CR1) in MC/MG obtained from IFN-γ and PBS-treated EAE mice by flow cytometry (Supplementary Figure 7A). Interestingly, we found that *in vivo* IFN-γ treatment induced a significantly higher expression of CX3CR1 in

MC/MG cells than in control cells (Figure 6A). In turn, an analysis of CX3CR1^{high}CD11b$^+$Ly6G$^-$ cells showed that IFN-γ treatment induced a significantly higher frequency of these cells expressing low PD-L1 (Figure 6B; Supplementary Figure 7B). There was no difference in the absolute number of CX3CR1^{high}PD-L1^{low}CD11b$^+$Ly6G$^-$ cells from mice treated with IFN-γ or PBS. However, the total number of live mononuclear cells isolated from the SC of IFN-γ-treated EAE mice was almost half of PBS-treated EAE mice (Figure 3A). These CX3CR1^{high}PD-L1^{low}CD11b$^+$Ly6G$^-$ cells were 75-85% TMEM119$^+$ (Supplementary Figure 8A). In addition, CX3CR1^{high}PD-L1^{low}CD11b$^+$Ly6G$^-$ cells showed a strong expression of gene markers for MG and weak expression for MC, oligodendrocytes, and astrocytes (Supplementary Figure 8B). Therefore, these results strongly suggest that this cell subpopulation is an enriched subset of CX3CR1^{high} MG expressing low PD-L1
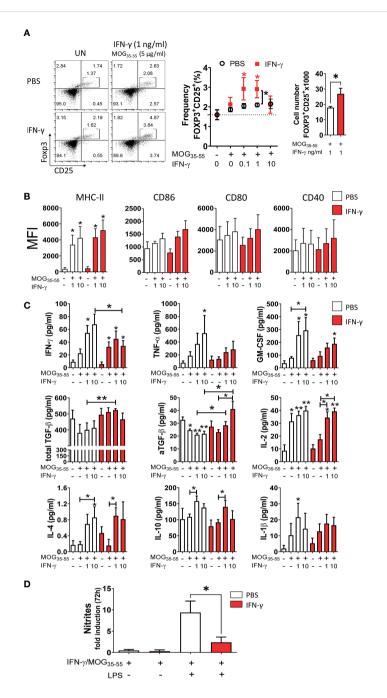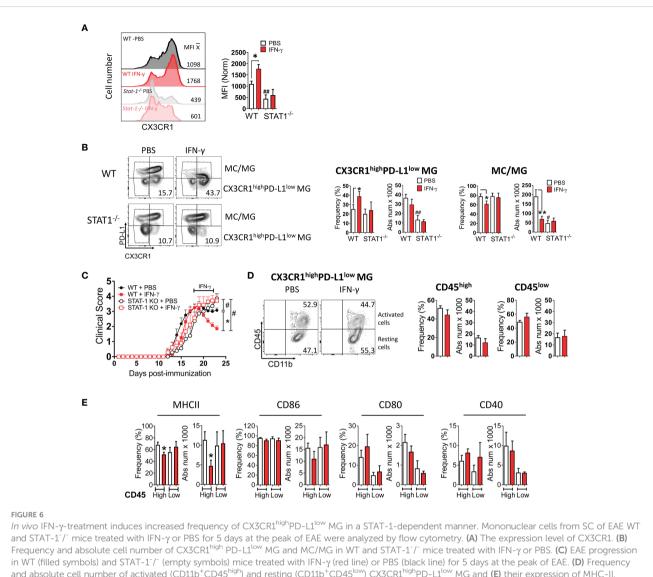
FIGURE 5

Ex vivo re-stimulation with low doses of IFN-γ and MOG₃₅-₅₅ induces tolerogenic activity in myeloid cell/microglia from IFN-γ-treated EAE mice.
(A) Primary MC/MG culture from EAE mice treated with IFN-γ (red squares) or PBS (white circles) were *ex vivo* pre-conditioned with low concentrations of IFN-γ (0.1, 1, and 10 ng/ml) for 24 h, incubated with 5 μg/ml MOG₃₅-₅₅ for an additional 24 h, and then co-cultured with purified CD4+ T cells obtained from spleens of transgenic 2D2 mice for 96 h. The frequency of Treg cells (CD4+CD25high FoxP3+) was determined by flow cytometry. Representative flow cytometry plots and frequency and cell number of Tregs in co-cultures containing untreated (UN) or pre-conditioned MC/MG with 1 ng/ml IFN-γ and 5 μg/ml MOG₃₅-₅₅ is shown. **(B)** The cell surface expression, shown as median fluorescence intensity (MFI), of MHC-II molecules, CD86, CD80, and CD40 was determined by flow cytometry in primary MC/MG obtained from EAE mice treated with IFN-γ (red bars) or PBS (white bars) and pre-conditioned with 1 or 10 ng/ml IFN-γ and 5 μg/ml MOG₃₅-₅₅ prior to culture with 2D2 CD4+ T cells. **(C)** Secretion of IFN-γ, TNF-α, GM-CSF, IL-2, IL-4, IL-10, and IL-1β was determined by multiplex assay and the production of TGF-β by ELISA in cell culture supernatants from co-cultures between 2D2 CD4+ T cells and pre-conditioned MC/MG. **(D)** Production of nitrites was determined by Griess assay in primary MC/MG obtained from EAE mice treated with IFN-γ (red bars) or PBS (white bars) pre-conditioned with 1 ng/ml IFN-γ and 5 μg/ml MOG₃₅-₅₅ (IFN-γ/MOG₃₅-₅₅) and challenged with 1 μg/ml LPS for 72 h. Results are shown as mean ± SEM of five independent experiments. *Comparison between unstimulated cell cultures and cell cultures stimulated with IFN-γ. Other relevant comparisons are shown with brackets. *P <0.05; **P <0.01. aTGF-β: active transforming growth factor.

FIGURE 6

In vivo IFN-γ-treatment induces increased frequency of CX3CR1^{high}PD-L1^{low} MG in a STAT-1-dependent manner. Mononuclear cells from SC of EAE WT and STAT-1$^{-/-}$ mice treated with IFN-γ or PBS for 5 days at the peak of EAE were analyzed by flow cytometry. **(A)** The expression level of CX3CR1. **(B)** Frequency and absolute cell number of CX3CR1^{high} PD-L1^{low} MG and MC/MG in WT and STAT-1$^{-/-}$ mice treated with IFN-γ or PBS. **(C)** EAE progression in WT (filled symbols) and STAT-1$^{-/-}$ (empty symbols) mice treated with IFN-γ (red line) or PBS (black line) for 5 days at the peak of EAE. **(D)** Frequency and absolute cell number of activated (CD11b$^+$CD45^{high}) and resting (CD11b$^+$CD45^{low}) CX3CR1^{high}PD-L1^{low} MG and **(E)** their expression of MHC-II, CD86, CD80, and CD40 molecules. *Comparison between mice or cells obtained from IFN-γ-treated EAE mice and control cells obtained from PBS-treated EAE mice. *P <0.05; **P <0.01. #Comparison between mice or cells obtained from WT and STAT1$^{-/-}$ mice. #P <0.05; ##P <0.01. MFI, median fluorescence intensity.

(CX3CR1^{high}PD-L1^{low} MG). The remaining cells were 47-52% TMEM119$^+$ (Supplementary Figure 8A) and were considered MC/MG. A significantly lower frequency and absolute number of MC/MG was observed in SC from IFN-γ-treated EAE mice than in SC from PBS-treated EAE mice (Figure 6B). Interestingly, NI mice exhibited a significantly higher frequency and absolute number of CX3CR1^{high}PD-L1^{low} MG (60.2% ± 5.4%) than MC/MG (39.5% ± 5.6%) (Supplementary Figure 9A).

To determine whether the increase in CX3CR1^{high}PD-L1^{low} MG induced by IFN-γ is due to proliferation, mice treated with IFN-γ or PBS received a simultaneous i.p. injection of 5-bromo-2′-deoxyuridine (BrdU) starting at the peak of EAE. After 5 days, mononuclear cells were isolated from SC, and the frequency of proliferating CX3CR1^{high}PD-L1^{low} MG was analyzed by flow cytometry. The results showed that there was no difference in the frequency of proliferating CX3CR1^{high}PD-L1^{low} MG between EAE mice treated with IFN-γ or PBS, suggesting that enhanced

CX3CR1^{high}PD-L1^{low} MG induced by IFN-γ might be explained by microglial plasticity (Supplementary Figure 9; Method S2).

To obtain mechanistic insight into the induction of CX3CR1^{high}PD-L1^{low} MG by IFN-γ, mice lacking STAT-1, the major STAT activated in response to engagement of IFN-γ receptor, were induced with EAE and then treated with IFN-γ for 5 days starting at the peak of disease. IFN-γ treatment had no effect on disease progression in EAE-induced *Stat*-1$^{-/-}$ mice (Figure 6C). Furthermore, the lack of STAT-1 inhibited the IFN-γ-induced expression of CX3CR1 in MC/MG cells (Figure 6A), suppressed the increase of CX3CR1^{high}PD-L1^{low} MG, and reversed the decreased frequency of MC/MG induced by IFN-γ in WT mice (Figure 6B). We thus conclude that the IFN-γ/STAT-1 signaling axis is involved in symptom amelioration and induction of CX3CR1^{high}PD-L1^{low} MG in EAE.

Next, we analyzed the impact of IFN-γ-treatment on the activation state and the expression of MHC-II molecules and costimulatory molecules in CX3CR1^{high}PD-L1^{low} MG from EAE-

induced WT mice treated with IFN-γ or PBS. A similar frequency of activated (51.5 ± 6%) and resting (44.2 ± 12%) CX3CR1^highPD-L1^low MG was found in SC from IFN-γ- and PBS-treated EAE mice (Figure 6D). However, activated CX3CR1^highPD-L1^low MG from IFN-γ-treated EAE mice exhibited a significantly lower frequency and absolute number of cells expressing MHC-II molecules than cells from PBS-treated EAE mice (Figure 6E). There was no significant difference in the frequency or absolute number of cells expressing CD80, CD86, or CD40 between CX3CR1^highPD-L1^low MG from IFN-γ- and PBS-treated EAE mice. Interestingly, in NI mice most of CX3CR1^highPD-L1^low MG (91.9% ± 4.2%) were in a resting state and had significantly lower frequency of cells expressing CD40 compared to activated cells, whereas the expression of MHC-II molecules, CD86, and CD80 were not statistically significant (Supplementary Figure 9B).

3.4 Differential gene expression profile of MG isolated from IFN-γ or PBS-treated EAE mice

We next wanted to identify genes and signaling pathways in which IFN-γ may be differentially regulating the activity of CX3CR1^highPD-L1^low MG in EAE by analyzing the transcriptional profile of these cells. CX3CR1^highPD-L1^low MG were isolated from IFN-γ- and PBS-treated EAE mice for FACS sorter (97.5% purity), and the transcriptional profile was analyzed by RNAseq. A total of 12,524 genes were detected above the threshold (see Methods), with 336 genes upregulated and 188 down-regulated after IFN-γ treatment (Figure 7A). Using more stringent criteria, lowering the p-value to 0.01, setting the Log2 Fold change to a minimum of 1.0, and raising the threshold of minimum expression to 40 read units,
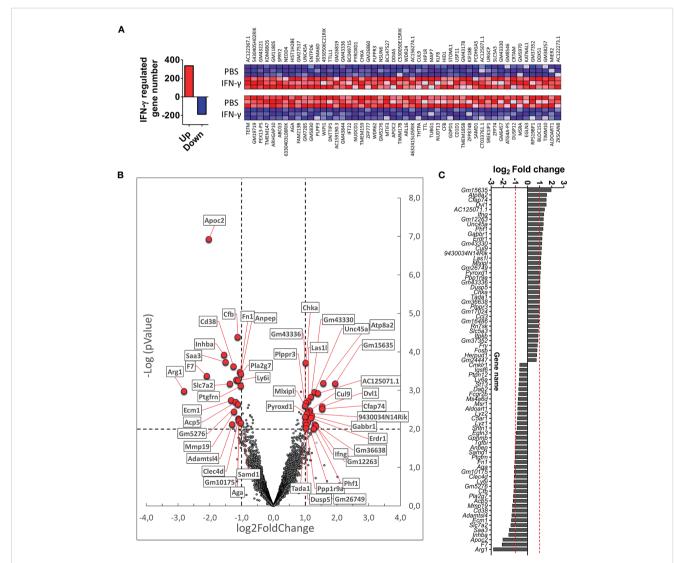

FIGURE 7

Differential gene expression profile in CX3CR1^highPD-L1^low MG in response to *in vivo* IFN-γ-treatment. Gene expression profile was analyzed on RNA obtained from CX3CR1^high MG expressing low PD-L1 purified from SC of IFN-γ or PBS-treated EAE mice by RNA sequencing (RNA-seq). **(A)** Left panel, total number of genes up (red bar)- and down (blue bar)-regulated by IFN-γ treatment; right panel, heat map showing the top 100 up (red squares)- and down (blue squares)-regulated genes in CX3CR1^highPD-L1^low MG from IFN-γ-treated mice versus those cells from PBS-treated mice. **(B)** Volcano plot showing up- and down-regulated genes induced by IFN-γ in CX3CR1^highPD-L1^low MG from IFN-γ-treated mice. **(C)** Gene expression analysis using more stringent criteria by lowering the p-value to 0.01, setting the Log2 Fold change to a minimum of 1.0, and by raising the threshold of minimum expression to 40 units. n= 3 independent samples per group.

resulted in 25 upregulated and 22 down-regulated genes in response to IFN-γ (Figures 7B, C). Interestingly, the gene expression of *ATPase phospholipid transporting 8A2* (*Atp8a2*), a selective microglial gene marker, and several genes associated with anti-inflammatory processes such as *dual-specificity phosphatase 5* (*Dusp5*), *MLX interacting protein-like* (*Mlxipl, ChREBP*), *dishevelled segment polarity protein 1* (*Dvl1*) and *gamma-aminobutyric acid type B receptor subunit 1* (*Gabbr1*), were upregulated in IFN-γ-treated EAE CX3CR1^{high}PD-L1^{low} MG (Figures 7B, C; Table 2). Several genes associated with M1 inflammatory activity such as the *cd38 molecule* (*Cd38*), *complement factor B* (*Cfb*), *inhibin subunit Beta A* (*Inhba*), *serum amyloid A3* (*Saa3*), *and* APN-like peptidase cytosolic alanyl-aminopeptidase *(Anpep)* were down-regulated in IFN-γ-treated

EAE CX3CR1^{high}PD-L1^{low} MG (Figures 7B, C; Table 2). Unexpectedly, *arginase 1* (*Arg1*), a M2 classic gene, was down-regulated in CX3CR1^{high}PD-L1^{low} MG from IFN-γ-treated EAE mice. However, the cationic amino acid transporter 2 (*Slc7a2*), a gene involved in the uptake of arginine, was also down-regulated, suggesting a decreased substrate availability for NO production in these cells (Figures 7B, C; Table 2).

3.5 IFN-γ-treatment induces an anti-inflammatory profile in MG

To determine if any molecular pathways were differentially regulated in CX3CR1^{high}PD-L1^{low} MG by IFN-γ, changes in the

TABLE 2   Role of genes regulated by IFN-γ.

Up	Name	Activity	Role	Ref
Atp8a2	ATPase Phospholipid Transporting 8A2	Lipid flipping: generating and maintaining asymmetry in membrane lipid	Selective microglial marker	(117)
Dusp5	Dual specificity phosphatase 5	Mitogen-activated protein kinase phosphatase	Inhibits production of TNF-α and IL-6 by inactivating ERK 1/2 pathway	(61, 62)
Mixipl (ChREBP)	Carbohydrate-responsive element binding protein	Transcription factor involved in regulation and maintenance of macrophages redox status	Prevents macrophage inflammatory responses	(63)
Dvl1	Dishevelled Segment Polarity Protein 1	Cytoplasmic phosphoprotein	Participates in the Wnt/β-catenin signaling pathway inducing tolerogenic DC	(64, 65)
Gabbr1	Gamma-Aminobutyric Acid Type B Receptor Subunit 1	Metabotropic GABAB inhibitory G-coupled receptor	Inhibits LPS-induced IL-6 and IL-12p40 expression in microglia	(66, 67)
Ifn-y	Interferon-y	Cytokine	Pro- and anti-inflammatory role	(19)
Down	**Name**	**Activity**	**Role**	**Ref**
Cd38	CD38	Transmembrane enzyme that synthesizes and hydrolyzes cADP-ribose	Associated to M1 macrophages activity inducing activation of iNOS and production of TNF-α, IL-6 and IL-1β. EAE mice lacking CD38 showed ameliorated disease.	(68–71)
Cfb	Complement Factor B	Component of the alternative pathway complement activation	Associated to M1 macrophages activity. Enhanced expression of Cfb in microglia is associated with late stages of neurodegeneration. Inhibition of alternative complement pathway in EAE attenuated the chronic phase of disease.	(72)
Inhba	Inhibin Subunit Beta A (Activin A)	Member of TGF-β- superfamily proteins	Induces M1 macrophage polarization and is considered a canonical M1 marker. Blocking anti-Activin A antibody reduced M1 macrophage polarization	(73, 74)
Saa3	Serum amyloid A3	Acute phase lipoprotein	Associated to M1 macrophage activity. Considered a pro-inflammatory biomarker involved in releasing active IL-1β by the activation of the NLRP3 inflammasome in LPS-induced microglia	(75–77)
Anpep	Alanyl Aminopeptidase, membrane (CD13)	aminopeptidase	Involved in adhesion of monocytes to endothelial cells and trafficking toward inflammation. Pharmacological inhibition of ANPEP induced amelioration of EAE.	(110–111)
Slc7a2	Solute Carrier Family 7 Member 2 (CAT2)	Cationic amino acid transporter	Responsible for the cellular uptake of arginine, lysine, and ornithine. Controls critical aspects of macrophage activation	(78)
Arg 1	Arginase 1	Catalyzes the hydrolysis of arginine to ornithine	A canonical M2 marker	(73)

transcriptional profile were analyzed by gene set enrichment analysis (GSEA) using different reference databases. Using Gene Ontology (GO) biological processes and Reactome databases, we found that gene sets corresponding to RNA transcription and nucleus-cytoplasmatic transporter activity were highly and significantly upregulated in CX3CR1^highPD-L1^low MG from IFN-γ-treated EAE mice, compared to the control group (*p*< 0.001);

indicating enhanced transcriptional and translational activities in response to IFN-γ stimulation (Figure 8A). The Kyoto Encyclopedia of Genes and Genomes (KEGG) analysis showed that the top enriched gene set induced by IFN-γ were related to signaling transduction pathways (MAPK and RIG I like receptor), transcription factors (Basal transcription factors), and metabolism (Methionine and Glycerolipids metabolism), which might be

FIGURE 8

Gene set enrichment analysis (GSEA) and over-representation analysis in CX3CR1^highPD-L1^low MG in response to *in vivo* IFN-γ-treatment. GSEA enrichment score plots show **(A)** up-regulation of gene sets corresponding to RNA transcription and to nucleus-cytoplasmatic transporter activity in CX3CR1^highPD-L1^low MG from IFN-γ-treated EAE mice compared to those cells from PBS-treated EAE mice. Each bar at the bottom of each panel represents a member gene of the respective pathway and shows its relative location in the ranked list. **(B)** Normalized enrichment scores indicate the distribution of Gene Ontology categories across a list of genes ranked by hypergeometrical score (HGS). Higher enrichment scores indicate a shift of genes belonging to certain GO, KEGG, or Reactome categories toward either end of the ranked list, representing up or down-regulation (positive or negative values, respectively). **(C)** Over-representation analysis showing significantly up- and down-regulated cellular pathways in MG from IFN-γ-treated EAE mice compared to MG from PBS-treated EAE mice. n=3 independent samples per group.

related to a change in the activation pattern, oxidative status and lipid-related metabolism associated with a decreased inflammatory profile. Instead, downregulated enriched gene sets in CX3CR1^{high}PD-L1^{low} MG from IFN-γ-treated EAE mice were associated with oxidative metabolism (pyruvate metabolism), lipid metabolism, nitric oxide induction (peroxisome), and G-protein coupled receptor-associated to a neuroantigen response (neuroactive ligand-receptor interaction) (Figure 8B). Remarkably, over-representation analysis using the Reactome database showed that IFN-γ significantly induced an anti-inflammatory profile in EAE MG. Regarding immune cell function, genes in the TRAF3-dependent IRF activation pathway and Interleukin-10 signaling pathway were upregulated, while neutrophil degranulation, alternative complement activation, and activation of C3 and C5 pathways were down-regulated in CX3CR1^{high}PD-L1^{low} MG from IFN-γ-treated EAE mice (Figure 8C). Taken together, these results confirm that IFN-γ is a key inducer of anti-inflammatory pathways and suppressor of inflammatory mechanisms in EAE MG.

Because our results indicate the importance of IFN-γ/STAT-1 axis in the induction of CX3CR1^{high}PD-L1^{low} MG in EAE, STAT-1 target genes were analyzed in our RNAseq database using the Harmonizome database (p< 0.05) (79). The analysis revealed that 8 genes (*Cfb, Dusp5, Anxa4, Neurl1b, C3, Naca, Anxa11, Slc15a2*) were regulated by STAT-1. Using more stringent criteria (p< 0.01), Cfb and Dusp5 were functionally associated with STAT-1.
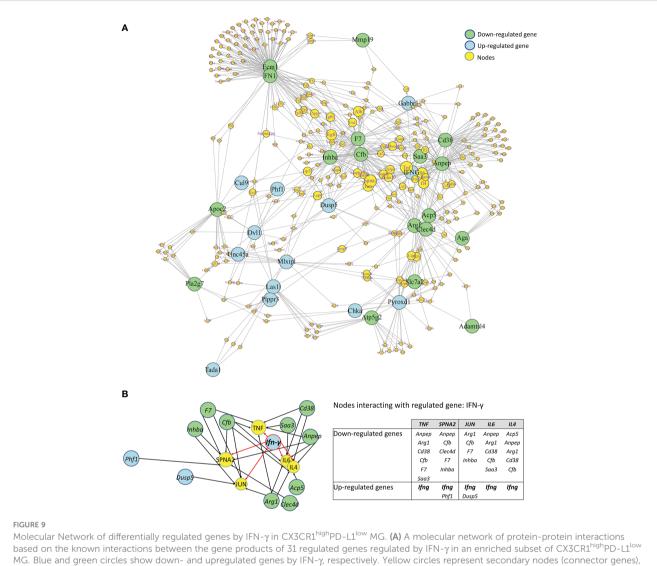
3.6 IFN-γ establishes tight connections with clusters of down-regulated inflammatory genes and with upregulated anti-inflammatory genes

In order to search for molecular connections among genes regulated by IFN-γ-treatment, a molecular network of protein-protein interactions has been constructed based on the known interactions between the gene products of the 25 up- and 22 down-regulated genes by IFN-γ using the STRING database. Some regulated genes could not be considered because no interacting proteins were found in the STRING database. This resulted in 31 regulated gene products (primary nodes), 13 up-regulated, and 18 down-regulated by IFN-γ-treatment, with various numbers – up to 100 – of interacting proteins (secondary nodes) with each primary node. All secondary nodes were then searched for their occurrence in columns of at least two regulated gene products (Figure 9A). Inserting edges (connections) of all primary nodes with secondary nodes identified in their respective columns gave rise to the molecular network displayed in Figure 9. As expected, *Ifn-γ* interacted with secondary nodes associated with inflammation, such as TNF-α, IL-6, IL-4, TGF-β1, or IL-10 (Figure 9A). Interestingly, we also found that *Ifn-γ* associated with secondary nodes interacting with three clusters of down-regulated inflammatory genes (cluster 1: *Inhba, Cfb, and F7; cluster 2: Saa3, Cd38, and Anpep; cluster 3: acid phosphatase 5, tartrate resistant (Acp5), c-type lectin domain family 4 member d (Clec4d), and Arg1*) and with secondary nodes interacting with up-regulated genes associated with anti-inflammatory roles (*Dusp5, Mlxipl, and Gabbr1*) (Figures 9A, B; Table 2).

4 Discussion

The role of IFN-γ in EAE and MS is still controversial, with evidence supporting both a pathogenic and beneficial function. Some studies have suggested that IFN-γ may have dual activity in these diseases depending on the dose, target cell, and stage of the disease [reviewed in (19–21)]. However, the neuroprotective mechanisms of IFN-γ in EAE remain largely unclear. It is shown here, for the first time, that IFN-γ has therapeutic activity at the peak of EAE by suppressing neuroinflammation and inducing tolerogenic activity of MC/MG and STAT-1-dependent homeostatic adaptation of MG.

Our results showed that IFN-γ-treatment resulted in a significant amelioration of clinical symptoms and reduction of body weight loss. Consistently, SC from IFN-γ-treated EAE mice had significantly less infiltration of inflammatory cells and fewer demyelinated areas. Furthermore, dampening of neuroinflammation by IFN-γ was associated with decreased frequency of CNS infiltrating CD11b$^+$ cells and activated MC/MG and increased frequency of resting MG. Decrease of absolute cell number of CD11b$^+$ cells was associated with a selective decrease in the absolute cell number of activated CD45^{high} cells without changes in the absolute cell number of resting CD45^{low} cells. This effect could reflect a decreased infiltration of peripheral MC, a deactivation of CD45^{high} activated MC/MG or both processes induced by treatment with IFN-γ. We have found no significant difference in the total numbers of cells in lymph nodes and spleen from IFN-γ- and PBS-treated EAE mice. However, splenic CD11b$^+$ cells and neutrophils were significantly reduced in EAE mice treated with IFN-γ; whilst macrophages were not significantly altered. Further studies will be necessary to determine if other peripheral subsets of CD11b$^+$ cells are influenced by IFN-γ. In addition, we have found a similar number of cells and frequencies of CD4$^+$ T cells, Th1, and Th17 cells in the periphery and the CNS of IFN-γ- and PBS-treated EAE mice (unpublished data). Although IFN-γ did not affect macrophages, these results suggest that IFN-γ might also have a protective role in EAE decreasing the abundance of neutrophils and some other peripheral subset of CD11b$^+$ cells, which might indirectly contribute to downregulate MG activation. However, induction of tolerogenic and anti-inflammatory activity in primary MC/MG cultures from the spinal cord of IFN-γ-treated EAE mice by *ex vivo* re-stimulation with low doses of IFN-γ and MOG$_{35-55}$ argues for a direct regulatory role of IFN-γ on these cells. Supporting this view, several studies have demonstrated a direct protective role of IFN-γ in the CNS as well as on MG. Intracerebroventricular (i.c.v.) administration of IFN-γ or intrathecal delivery of an IFN-γ expression system in EAE mice resulted in suppression of clinical symptoms (33, 34). *In vitro* assays have shown that IFN-γ treatment enabled MG to restore homeostasis by promoting neuroprotection, neurogenesis and glutamate clearance (80–82). In turn, i.c.v. injection of IFN-γ-treated MG during the inductive phase of EAE significantly delayed the onset of the disease compared to control mice (83). Remarkably, silencing IFN-γ signaling in MG significantly enhanced EAE severity accompanied by a significant increase in the total number mononuclear cells and in the absolute number of CD11b$^+$, CD11b$^+$CD45^{lo}, CD11b$^+$CD45^{high}, CD11c$^+$, Gr-1$^+$, CD4$^+$, Th1, and

FIGURE 9

Molecular Network of differentially regulated genes by IFN-γ in CX3CR1^{high}PD-L1^{low} MG. **(A)** A molecular network of protein-protein interactions based on the known interactions between the gene products of 31 regulated genes regulated by IFN-γ in an enriched subset of CX3CR1[high]PD-L1[low] MG. Blue and green circles show down- and upregulated genes by IFN-γ, respectively. Yellow circles represent secondary nodes (connector genes), and their size represents the number of connections with regulated genes. Lines indicate the interaction of regulated genes with connector genes. **(B)** An enlarged area of the molecular network showing that *Ifn-γ* associated with connectors (yellow circles) interacting with three clusters of down-regulated inflammatory genes (green circles) as well as with connectors interacting with upregulated genes (blue circles) associated with anti-inflammatory roles. The table summarizes the up- and down-regulated genes by IFN-γ that interact with each connector.

Th17 cells in both spinal cords and brainstems (84). These findings are consistent with our results showing that IFN-γ treatment significantly reduces the total number of mononuclear cells and CD11b^{+} cells in spinal cord of EAE mice and demonstrate that IFN-γ signaling in MG plays an important role in controlling CNS cell infiltration and MG activation. On the other hand, a previous report using bone marrow chimeras showed that the protective effect of IFN-γ in EAE is mediated by an increased production of nitric oxide (NO) at the level of both the periphery and the CNS. Peripheral mononuclear cells were identified as cells producing NO in the periphery whereas the authors suggested that microglia and astrocytes could be involved in the IFN-γ-driven NO production in the CNS (85). Taken together, the evidence suggests that IFN-γ can exert protective effects both in the periphery as in the CNS.

Importantly, immunohistochemistry analysis confirmed a significant increase in the percentage of resting microglia, characterized by a ramified morphology and reduced density and cell size, in response to IFN-γ. Furthermore, high expression of TMEM119, a homeostatic marker of MG, and of MBP1 was observed in the cerebellum from IFN-γ-treated EAE mice, supporting the notion that IFN-γ induces a shift of activated MG to a homeostatic profile. These results are in line with previous observations showing that IFN-γ plays an important role in EAE; regulating inflammation of specific regions of the CNS (55–57, 86).

Ex vivo re-stimulation with low doses of IFN-γ (1 ng/ml) and MOG$_{35-55}$ of primary MC/MG cultures obtained from IFN-γ-treated EAE mice resulted in conversion of CD4^{+} T cells into Treg cells associated with higher secretion of TGF-β. Consistently, we have found a significant increase of Treg cells in spinal cord from IFN-γ-treated EAE mice compared to that of the PBS-treated EAE mice (unpublished data). In line with our results, low concentrations of IFN-γ induce a tolerogenic phenotype in MG

from neonatal mice, characterized by the expression of intermediate levels of MHC-II and increased secretion of IL-10, capable of inducing Treg cells (59). Supporting our results, a recent study showed that microglia require IFN-γ-signaling to shape the Treg cell compartment in relapsing-remitting EAE and that the absence of microglial IFN-γ-receptor results in worse disease (87). Another study showed that the administration of the microparticle MIS416 in EAE mice induced an IFN-γ-dependent expansion and suppressive function of Treg cells (88). Additionally, a direct role of IFN-γ on the conversion of CD4$^+$CD25$^-$ T cells to CD4$^+$ Treg cells has been reported in EAE (89). Taken together, these results suggest that IFN-γ exerts a tolerogenic role in EAE acting on Treg cells either directly or indirectly through MC/MG.

The contribution of Treg cells to the mechanisms that actively regulate the neuroinflammatory process in EAE has been unequivocally demonstrated (90, 91). Different treatments such as glatiramer acetate, indoleamine 2,3-dioxygenase (IDO), and IL-10 administration, suppress EAE progression promoting an increase in Treg cells (92, 93). In contrast, other treatments such as atorvastatin and trichostatin A suppress EAE progression in a Treg cell-independent manner, suggesting that Treg cells may not always be necessary for the protective effects of some treatments for EAE (94–96). In addition, Korn et al. reported that Treg cells expand in the periphery and accumulate in the CNS but are unable to suppress the proliferation of MOG$_{35-55}$-specific T effector cells from the CNS. Intrinsic resistance of CNS-derived T effector cells to suppression was associated with high production of IL-6 and TNF (97, 98). However, a subsequent report combining targeted depletion of Treg cells with intravital two-photon microscopy concluded that Treg cells mediate recovery from EAE by controlling cytokine production, proliferation, and motility of effector T cells in the CNS (99). Therefore, the activity of Treg cells can be understood as a dynamic process that would depend on the balance between Treg cells and effector T cells as well as the local inflammatory cytokine milieu (90). Additionally, crosstalk between Treg cells and local APC might be critical in modulating effector T cell pathogenicity (100). Our results showing a higher production of TGF-β and conversion of Treg cells in IFN-γ-treated primary MC/MG cultures obtained from IFN-γ-treated EAE mice are consistent with that model of regulation.

We found that MC/MG from EAE mice treated with IFN-γ had a higher expression of CX3CR1, in support of a recent study showing high expression of CX3CR1 in MG at the peak of EAE (10). CX3CR1 is highly expressed in MG (101, 102) as an alert receptor "sensing" the ligand CX3CL1 released by dying neurons. Importantly, lack of this receptor exacerbates inflammation and increases the expression of MHC class II molecules in microglial cells (12–14). In addition, we found that IFN-γ induced a higher frequency of MG with high expression of CX3CR1 and low expression of PD-L1, compared to MG obtained from PBS-treated EAE mice. Although PD-L1 is involved in maintaining immune tolerance and homeostasis through the regulation of T cell activation and differentiation in MS and EAE (103), low expression or absence of PD-L1 has also been related to a tolerogenic effect of APC. Consistent with our findings, low doses of IFN-γ were required to obtain optimal activation of type II macrophages, a

subset of macrophages that have been shown to induce a Th2-type anti-inflammatory response after initial activation in an inflammatory environment. Interestingly, IFN-γ-primed type II-macrophages are characterized by an enhanced production of IL-10, reduced expression of IL-12, and low expression of PD-L1, CD40, and CD80. Furthermore, mice receiving IFN-γ-primed type II-activated macrophages were protected from EAE whereas those receiving classically activated macrophages developed EAE (104). In another study, TNF-treated semi-mature DC deficient in PD-L1 showed a stronger tolerogenic capacity in EAE protection compared to wild-type DC. PD-L1$^{-/-}$DC-treated EAE mice presented lower numbers of MOG-specific IFN-γ and IL-17 producing cells in the CNS whereas an increased production of the protective cytokines IL-10, IL-13, and IL-4, and reduced levels of IFN-γ and IL-17 were detected in the periphery. Therefore, absence of PD-L1 expression on semi-mature DC enhanced their tolerogenic activity in EAE mice (105).

Bulk RNAseq analysis and recent single-cell RNAseq studies of MG have revealed that unique MG subpopulations, characterized by a distinct signature, emerge during development and homeostasis in the healthy brain as well as during demyelination and remyelination in models of demyelinating and neurodegenerative diseases, including EAE and MS (106–108). These results confirm the ability of MG to shift into different functional states in response to a variety of environmental challenges. Accordingly, our results uncover a new mechanism whereby IFN-γ enables a subset of MG to adapt the transcriptional program into a tolerogenic and anti-inflammatory profile at the peak of EAE. Transcriptional profile analysis of CX3CR1^{high}PD-L1^{low} MG isolated from IFN-γ- and PBS-treated EAE mice revealed that genes with a pro-inflammatory role in MC, MG and EAE such as *Cd38* (68–71, 109), *Cfb* (72, 108), *Saa3* (75, 76), *Inhba, Anpep* (110, 111), and *Apoc2* (112) were down-regulated by IFN-γ. From these genes, *Cd38, Cfb, Saa3, and Inhba* are considered canonical M1 pro-inflammatory genes in macrophages (73, 74). Transcriptional analysis of MG have showed that genes encoding for apolipoprotein C1 and C2 (*Apoc1* and *Apoc2*) were up-regulated during the process of demyelination in the mouse cuprizone model and brain samples from MS patients (107, 112). Interestingly, IFN-γ treatment induced a down-regulation of *Apoc2* in CX3CR1^{high}PD-L1^{low} MG. Taken together, these results highlight lipid and lipoprotein metabolism as a key mechanism in the modulation of microglial inflammatory status and as a modifiable target for the treatment of MS (113). A significantly lower frequency and absolute number of activated CX3CR1^{high}PD-L1^{low} MG expressing MHC-II molecules was found in IFN-γ-treated EAE mice but not in MG from PBS-treated EAE mice. In addition, a decreased expression of MHC class II antigen presentation gene set was observed in CX3CR1^{high}PD-L1^{low} MG from IFN-γ-treated EAE mice compared with CX3CR1^{high}PD-L1^{low} MG from control mice; although this difference did not reach statistical significance. Also, *Cfb*, a component of the alternative pathway of complement activation, was downregulated in CX3CR1^{high}PD-L1^{low} MG from IFN-γ-treated EAE mice. Consistent with our results, single-cell RNAseq analysis revealed decreased gene expression of the MHC-II antigen presentation

pathway both in peripheral APC (dendritic cells, macrophages and B cells) as in microglia in EAE mice treated at the peak of disease with an antigen-specific dual microparticle system (Ag-dMP). In addition, a set of complement genes were downregulated in the microglia from Ag-dMP-treated EAE mice (114). Consequently, EAE mice treated with a monoclonal antibody directed against Cfb significantly attenuated the chronic phase of disease, resulting in reduced cellular infiltration, inflammation and demyelination (72). In line with these results, upregulation in the expression of complement components, including Cfb and MHC-II pathway was determined by single-cell RNAseq analysis in MG isolated during the later stages of neurodegeneration in an Alzheimer's disease-like animal model (108). Arginase 1 (Arg-1) is an enzyme dominantly expressed in M2 macrophages that hydrolyzes arginine to ornithine and urea, limiting bioavailability of intracellular arginine to be metabolized to NO by the enzyme nitric oxide synthase (NOS), resulting in dampening of inflammation (115, 116). Surprisingly, we found that *Arg1*, encoding arginase 1, was down-regulated in CX3CR1^{high}PD-L1^{low} MG by IFN-γ treatment. However, *Nos2*, encoding inducible NOS, was slightly decreased. In addition, *Slc7a2*, which encodes inducible cationic amino acid transporter, and is involved in the uptake of arginine (78), was significantly down-regulated. Consequently, decreased availability of arginine could be expected in response to IFN-γ treatment. Therefore, although *Arg1* is down-regulated in CX3CR1^{high}PD-L1^{low} MG, the net result would be an anti-inflammatory effect due to a decrease in the uptake of arginine and decreased *Nos2* expression. This hypothesis is supported by the decreased secretion of nitrites induced by LPS in primary MC/MG cell cultures obtained from IFN-γ-treated EAE mice (Figure 5D). On the other hand, *Atp8a2* gene, a selective microglial marker (117), and other genes related to tolerogenic and anti-inflammatory processes in MG and EAE such as DVL-1 (64, 65) and Dusp5 (61, 62) were up-regulated by IFN-γ in CX3CR1^{high}PD-L1^{low} MG. Importantly, raising the Log2 Fold change to 1.5, a set of key genes (*Saa3, Inhba*, *Apoc2, Atp8a2, and* DVL-1) maintains differential expression in response to IFN-γ treatment.

Our results show that IFN-γ is unable to promote amelioration of EAE symptoms and induction of CX3CR1^{high}PD-L1^{low} MG in the absence of STAT-1, indicating that STAT-1 is critical in the protective effects mediated by IFN-γ in EAE. In line with these results, we found that from all up- and down-regulated genes in CX3CR1^{high}PD-L1^{low} MG by IFN-γ, 8 of them (*Cfb, Dusp5, Anxa4, Neurl1b, C3, Naca, Anxa11, Slc15a2*) are also regulated by STAT-1, suggesting that the IFN-γ/STAT-1 signaling axis would be involved in suppressing neuroinflammation in EAE regulating the expression of a set of genes involved in microglial activation. Supporting this potential mechanism, previous studies have reported that the IFN-γ/STAT-1 axis regulates the expression of indoleamine 2,3-dioxygenase (IDO), a tryptophan catabolizing enzyme involved in immune tolerance and suppression of EAE (118, 119), in microglia (120). Similarly, the IFN-γ/STAT-1 axis also regulates the tolerogenic activity of IDO in dendritic cells in a mouse model of prediabetes (121).

To obtain more detailed insights into the molecular interactions between the differentially expressed genes in MG in response to

IFN-γ, we created a molecular network of protein-protein interactions based on the known interactions between the products of the genes targeted by IFN-γ. In this analysis, the number of interacting genes depended on the existing knowledge available from the STRING database and does not necessarily reflect the actual number of biological interactions. Therefore, this model is biased as some genes have been widely studied by many investigators, others less so. Despite this, the model reveals molecules physiologically interacting with those identified by expression profiling and delivers a more complete understanding of their connectedness. These analyses highlight the master role that IFN-γ plays in regulating microglial activity and provide new insights into the cellular and molecular mechanisms involved in the therapeutic activity of IFN-γ in EAE.

5 Conclusions

Our findings show that IFN-γ exerts therapeutic activity in EAE by regulating myeloid cell infiltration and inducing attenuation of neuroinflammation and a shift from activated MG to resting MG. In addition, IFN-γ promotes the induction of homeostatic CX3CR1^{high}PD-L1^{low} MG, characterized by a homeostatic and anti-inflammatory transcriptional signature. The amelioration of clinical symptoms and the induction of CX3CR1^{high}PD-L1^{low} MG were dependent on STAT-1. Also, our analyses reveal that IFN-γ plays a master role in regulating a network of genes involved in microglial activation. Taken together, our findings uncover a novel cellular and molecular mechanism whereby IFN-γ exerts therapeutic activity in EAE and contribute to clarify the complex role that IFN-γ plays in EAE and MS.

Data availability statement

The RNA sequencing datasets generated for this study have been deposited in the NCBI GEO database under accession number GSE231833.

Ethics statement

The animal study was reviewed and approved by the Institutional Animal Care and Use Committee (IACUC) of the University of Chile and Northwestern University.

Author contributions

JT and RN conceived the project. JT, EA, GA, LG, PM, CP, JI-V, and EL performed the experiments and analysis of the data. MR and NK performed RNA-seq analysis. PG-H performed molecular network analysis and its interpretation. RN, JT, PG-H, PIB, SM discussed the results and wrote the manuscript. All authors contributed to the article and approved the submitted version.

Funding

Acknowledgments

Conflict of interest

The authors declare that the research was conducted in the absence of any commercial or financial relationships that could be construed as a potential conflict of interest.

Publisher's note

All claims expressed in this article are solely those of the authors and do not necessarily represent those of their affiliated organizations, or those of the publisher, the editors and the reviewers. Any product that may be evaluated in this article, or claim that may be made by its manufacturer, is not guaranteed or endorsed by the publisher.

Supplementary material

The Supplementary Material for this article can be found online at: https://www.frontiersin.org/articles/10.3389/fimmu.2023.1191838/full#supplementary-material

References

1. Dendrou CA, Fugger L, Friese MA. Immunopathology of multiple sclerosis. *Nat Rev Immunol* (2015) 15(9):545–58. doi: 10.1038/nri3871

2. Constantinescu CS, Farooqi N, O'Brien K, Gran B. Experimental autoimmune encephalomyelitis (Eae) as a model for multiple sclerosis (Ms). *Br J Pharmacol* (2011) 164(4):1079–106. doi: 10.1111/j.1476-5381.2011.01302.x

3. Miller SD, Karpus WJ. Experimental autoimmune encephalomyelitis in the mouse. *Curr Protoc Immunol* (2007) 77:15.1.1–15.1.18. doi: 10.1002/0471142735.im1501s77

4. Robinson AP, Harp CT, Noronha A, Miller SD. The experimental autoimmune encephalomyelitis (Eae) model of Ms: utility for understanding disease pathophysiology and treatment. *Handb Clin Neurol* (2014) 122:173–89. doi: 10.1016/b978-0-444-52001-2.00008-x

5. Greter M, Lelios I, Croxford AL. Microglia versus myeloid cell nomenclature during brain inflammation. *Front Immunol* (2015) 6:249. doi: 10.3389/fimmu.2015.00249

6. London A, Cohen M, Schwartz M. Microglia and monocyte-derived macrophages: functionally distinct populations that act in concert in cns plasticity and repair. *Front Cell Neurosci* (2013) 7:34. doi: 10.3389/fncel.2013.00034

7. Cardona AE, Pioro EP, Sasse ME, Kostenko V, Cardona SM, Dijkstra IM, et al. Control of microglial neurotoxicity by the fractalkine receptor. *Nat Neurosci* (2006) 9(7):917–24. doi: 10.1038/nn1715

8. Jung S, Aliberti J, Graemmel P, Sunshine MJ, Kreutzberg GW, Sher A, et al. Analysis of fractalkine receptor Cx(3)Cr1 function by targeted deletion and green fluorescent protein reporter gene insertion. *Mol Cell Biol* (2000) 20(11):4106–14. doi: 10.1128/mcb.20.11.4106-4114.2000

9. Wolf Y, Yona S, Kim KW, Jung S. Microglia, seen from the Cx3cr1 angle. *Front Cell Neurosci* (2013) 7:26. doi: 10.3389/fncel.2013.00026

10. Mrdjen D, Pavlovic A, Hartmann FJ, Schreiner B, Utz SG, Leung BP, et al. High-dimensional single-cell mapping of central nervous system immune cells reveals distinct myeloid subsets in health, aging, and disease. *Immunity* (2018) 48(3):599. doi: 10.1016/j.immuni.2018.02.014

11. Keren-Shaul H, Spinrad A, Weiner A, Matcovitch-Natan O, Dvir-Szternfeld R, Ulland TK, et al. A unique microglia type associated with restricting development of alzheimer's disease. *Cell* (2017) 169(7):1276–90 e17. doi: 10.1016/j.cell.2017.05.018

12. Breen KT, Anderson SR, Steele MR, Calkins DJ, Bosco A, Vetter ML. Loss of fractalkine signaling exacerbates axon transport dysfunction in a chronic model of glaucoma. *Front Neurosci* (2016) 10:526. doi: 10.3389/fnins.2016.00526

13. Feng X, Szulzewsky F, Yerevanian A, Chen Z, Heinzmann D, Rasmussen RD, et al. Loss of Cx3cr1 increases accumulation of inflammatory monocytes and promotes gliomagenesis. *Oncotarget* (2015) 6(17):15077–94. doi: 10.18632/oncotarget.3730

14. Mai W, Liu X, Wang J, Zheng J, Wang X, Zhou W. Protective effects of Cx3cr1 on autoimmune inflammation in a chronic eae model for Ms through modulation of

antigen-presenting cell-related molecular mhc-ii and its regulators. *Neurological Sci* (2019) 40(4):779–91. doi: 10.1007/s10072-019-3721-2

15. Zrzavy T, Hametner S, Wimmer I, Butovsky O, Weiner HL, Lassmann H. Loss of 'Homeostatic' microglia and patterns of their activation in active multiple sclerosis. *Brain* (2017) 140(7):1900–13. doi: 10.1093/brain/awx113

16. Plastini MJ, Desu HL, Brambilla R. Dynamic responses of microglia in animal models of multiple sclerosis. *Front Cell Neurosci* (2020) 14:269. doi: 10.3389/fncel.2020.00269

17. Deczkowska A, Baruch K, Schwartz M. Type I/Ii interferon balance in the regulation of brain physiology and pathology. *Trends Immunol* (2016) 37(3):181–92. doi: 10.1016/j.it.2016.01.006

18. Lowther DE, Chong DL, Ascough S, Ettorre A, Ingram RJ, Boyton RJ, et al. Th1 not Th17 cells drive spontaneous Ms-like disease despite a functional regulatory T cell response. *Acta neuropathologica* (2013) 126(4):501–15. doi: 10.1007/s00401-013-1159-9

19. Arellano G, Ottum PA, Reyes LI, Burgos PI, Naves R. Stage-specific role of interferon-gamma in experimental autoimmune encephalomyelitis and multiple sclerosis. *Front Immunol* (2015) 6:492. doi: 10.3389/fimmu.2015.00492

20. Ottum PA, Arellano G, Reyes LI, Iruretagoyena M, Naves R. Opposing roles of interferon-gamma on cells of the central nervous system in autoimmune neuroinflammation. *Front Immunol* (2015) 6:539. doi: 10.3389/fimmu.2015.00539

21. Sanvito L, Constantinescu CS, Gran B, t`Hart B. The multifaceted role of interferon-gamma in central nervous system autoimmune demyelination. *Open Autoimmun J* (2010) 2:151–9. doi: 10.2174/1876894601002040151

22. Krakowski M, Owens T. Interferon-gamma confers resistance to experimental allergic encephalomyelitis. *Eur J Immunol* (1996) 26(7):1641–6. doi: 10.1002/eji.1830260735

23. Sabatino JJJr., Shires J, Altman JD, Ford ML, Evavold BD. Loss of ifn-gamma enables the expansion of autoreactive Cd4+ T cells to induce experimental autoimmune encephalomyelitis by a nonencephalitogenic myelin variant antigen. *J Immunol* (2008) 180(7):4451–7. doi: 10.4049/jimmunol.180.7.4451

24. Ferber IA, Brocke S, Taylor-Edwards C, Ridgway W, Dinisco C, Steinman L, et al. Mice with a disrupted ifn-gamma gene are susceptible to the induction of experimental autoimmune encephalomyelitis (Eae). *J Immunol* (1996) 156(1):5–7. doi: 10.4049/jimmunol.156.1.5

25. Willenborg DO, Fordham S, Bernard CC, Cowden WB, Ramshaw IA. Ifn-gamma plays a critical down-regulatory role in the induction and effector phase of myelin oligodendrocyte glycoprotein-induced autoimmune encephalomyelitis. *J Immunol* (1996) 157(8):3223–7. doi: 10.4049/jimmunol.157.8.3223

26. Naves R, Singh SP, Cashman KS, Rowse AL, Axtell RC, Steinman L, et al. The interdependent, overlapping, and differential roles of type I and ii ifns in the

pathogenesis of experimental autoimmune encephalomyelitis. *J Immunol* (2013) 191 (6):2967–77. doi: 10.4049/jimmunol.1300419

27. Xiao BG, Ma CG, Xu LY, Link H, Lu CZ. Il-12/Ifn-Gamma/No axis plays critical role in development of Th1-mediated experimental autoimmune encephalomyelitis. *Mol Immunol* (2008) 45(4):1191–6. doi: 10.1016/j.molimm.2007.07.003

28. Billiau A, Heremans H, Vandekerckhove F, Dijkmans R, Sobis H, Meulepas E, et al. Enhancement of experimental allergic encephalomyelitis in mice by antibodies against ifn-gamma. *J Immunol* (1988) 140(5):1506–10. doi: 10.4049/jimmunol.140.5.1506

29. Lublin FD, Knobler RL, Kalman B, Goldhaber M, Marini J, Perrault M, et al. Monoclonal anti-gamma interferon antibodies enhance experimental allergic encephalomyelitis. *Autoimmunity* (1993) 16(4):267–74. doi: 10.3109/08916939309014645

30. Heremans H, Dillen C, Groenen M, Martens E, Billiau A. Chronic relapsing experimental autoimmune encephalomyelitis (Creae) in mice: enhancement by monoclonal antibodies against interferon-gamma. *Eur J Immunol* (1996) 26 (10):2393–8. doi: 10.1002/eji.1830261019

31. Duong TT, Finkelman FD, Singh B, Strejan GH. Effect of anti-Interferon-Gamma monoclonal antibody treatment on the development of experimental allergic encephalomyelitis in resistant mouse strains. *J neuroimmunology* (1994) 53(1):101–7. doi: 10.1016/0165-5728(94)90069-8

32. Dungan LS, McGuinness NC, Boon L, Lynch MA, Mills KHG. Innate ifn-gamma promotes development of experimental autoimmune encephalomyelitis: a role for nk cells and M1 macrophages. *Eur J Immunol* (2014) 44(10):2903–17. doi: 10.1002/eji.201444612

33. Voorthuis JA, Uitdehaag BM, De Groot CJ, Goede PH, van der Meide PH, Dijkstra CD. Suppression of experimental allergic encephalomyelitis by intraventricular administration of interferon-gamma in Lewis rats. *Clin Exp Immunol* (1990) 81(2):183–8. doi: 10.1111/j.1365-2249.1990.tb03315.x

34. Furlan R, Brambilla E, Ruffini F, Poliani PL, Bergami A, Marconi PC, et al. Intrathecal delivery of ifn-gamma protects C57bl/6 mice from chronic-progressive experimental autoimmune encephalomyelitis by increasing apoptosis of central nervous system-infiltrating lymphocytes. *J Immunol* (2001) 167(3):1821–9. doi: 10.4049/jimmunol.167.3.1821

35. Tanuma N, Shin T, Kogure K, Matsumoto Y. Differential role of tnf-alpha and ifn-gamma in the brain of rats with chronic relapsing autoimmune encephalomyelitis. *J neuroimmunology* (1999) 96(1):73–9. doi: 10.1016/s0165-5728(99)00018-1

36. Rowse AL, Naves R, Cashman KS, McGuire DJ, Mbana T, Raman C, et al. Lithium controls central nervous system autoimmunity through modulation of ifn-Γ signaling. *PloS One* (2012) 7(12):e52658. doi: 10.1371/journal.pone.0052658

37. Sedgwick JD, Schwender S, Imrich H, Dörries R, Butcher GW, ter Meulen V. Isolation and direct characterization of resident microglial cells from the normal and inflamed central nervous system. *Proc Natl Acad Sci United States America* (1991) 88 (16):7438–42. doi: 10.1073/pnas.88.16.7438

38. Love MI, Huber W, Anders S. Moderated estimation of fold change and dispersion for rna-seq data with Deseq2. *Genome Biol* (2014) 15(12):550. doi: 10.1186/s13059-014-0550-8

39. Wang J, Vasaikar S, Shi Z, Greer M, Zhang B. Webgestalt 2017: a more comprehensive, powerful, flexible and interactive gene set enrichment analysis toolkit. *Nucleic Acids Res* (2017) 45(W1):W130–W7. doi: 10.1093/nar/gkx356

40. Croft D, O'Kelly G, Wu G, Haw R, Gillespie M, Matthews L, et al. Reactome: a database of reactions, pathways and biological processes. *Nucleic Acids Res* (2011) 39 (Database issue):D691–7. doi: 10.1093/nar/gkq1018

41. Ford AL, Goodsall AL, Hickey WF, Sedgwick JD. Normal adult ramified microglia separated from other central nervous system macrophages by flow cytometric sorting. phenotypic differences defined and direct ex vivo antigen presentation to myelin basic protein-reactive Cd4+ T cells compared. *J Immunol* (1995) 154(9):4309–21. doi: 10.4049/jimmunol.154.9.4309

42. Martin E, El-Behi M, Fontaine B, Delarasse C. Analysis of microglia and monocyte-derived macrophages from the central nervous system by flow cytometry. *J visualized experiments JoVE* (2017) 124). doi: 10.3791/55781

43. Sedgwick JD, Ford AL, Foulcher E, Airriess R. Central nervous system microglial cell activation and proliferation follows direct interaction with tissue-infiltrating T cell blasts. *J Immunol* (1998) 160(11):5320–30. doi: 10.4049/jimmunol.160.11.5320

44. Muller A, Brandenburg S, Turkowski K, Muller S, Vajkoczy P. Resident microglia, and not peripheral macrophages, are the main source of brain tumor mononuclear cells. *Int J Cancer* (2015) 137(2):278–88. doi: 10.1002/ijc.29379

45. Mathur V, Burai R, Vest RT, Bonanno LN, Lehallier B, Zardeneta ME, et al. Activation of the sting-dependent type I interferon response reduces microglial reactivity and neuroinflammation. *Neuron* (2017) 96(6):1290–302 e6. doi: 10.1016/j.neuron.2017.11.032

46. Ponomarev ED, Shriver LP, Dittel BN. Cd40 expression by microglial cells is required for their completion of a two-step activation process during central nervous system autoimmune inflammation. *J Immunol* (2006) 176(3):1402–10. doi: 10.4049/jimmunol.176.3.1402

47. Mizutani M, Pino PA, Saederup N, Charo IF, Ransohoff RM, Cardona AE. The fractalkine receptor but not Ccr2 is present on microglia from embryonic development throughout adulthood. *J Immunol* (2012) 188(1):29–36. doi: 10.4049/jimmunol.1100421

48. Bennett ML, Bennett FC, Liddelow SA, Ajami B, Zamanian JL, Fernhoff NB, et al. New tools for studying microglia in the mouse and human cns. *Proc Natl Acad Sci United States America* (2016) 113(12):E1738–46. doi: 10.1073/pnas.1525528113

49. Ponomarev ED, Shriver LP, Maresz K, Dittel BN. Microglial cell activation and proliferation precedes the onset of cns autoimmunity. *J Neurosci Res* (2005) 81(3):374–89. doi: 10.1002/jnr.20488

50. Rooney S, Sah A, Unger MS, Kharitonova M, Sartori SB, Schwarzer C, et al. Neuroinflammatory alterations in trait anxiety: modulatory effects of minocycline. *Trans Psychiatry* (2020) 10(1):256. doi: 10.1038/s41398-020-00942-y

51. Gentile A, Rossi S, Studer V, Motta C, De Chiara V, Musella A, et al. Glatiramer acetate protects against inflammatory synaptopathy in experimental autoimmune encephalomyelitis. *J Neuroimmune Pharmacol* (2013) 8(3):651–63. doi: 10.1007/s11481-013-9436-x

52. Kozlowski C, Weimer RM. An automated method to quantify microglia morphology and application to monitor activation state longitudinally in vivo. *PloS One* (2012) 7(2):e31814. doi: 10.1371/journal.pone.0031814

53. Hovens IB, Nyakas C, Schoemaker RG. A novel method for evaluating microglial activation using ionized calcium-binding adaptor protein-1 staining: cell body to cell size ratio. *Neuroimmunology Neuroinflamm* (2014) 1:82–8. doi: 10.4103/2347-8659.139719

54. Sloka S, Metz LM, Hader W, Starreveld Y, Yong VW. Reduction of microglial activity in a model of multiple sclerosis by dipyridamole. *J Neuroinflamm* (2013) 10:89. doi: 10.1186/1742-2094-10-89

55. Wensky AK, Furtado GC, Marcondes MC, Chen S, Manfra D, Lira SA, et al. Ifn-gamma determines distinct clinical outcomes in autoimmune encephalomyelitis. *J Immunol* (2005) 174(3):1416–23. doi: 10.4049/jimmunol.174.3.1416

56. Stromnes IM, Cerretti LM, Liggitt D, Harris RA, Goverman JM. Differential regulation of central nervous system autoimmunity by T(H)1 and T(H)17 cells. *Nat Med* (2008) 14(3):337–42. doi: 10.1038/nm1715

57. Lees JR, Iwakura Y, Russell JH. Host T cells are the main producers of il-17 within the central nervous system during initiation of experimental autoimmune encephalomyelitis induced by adoptive transfer of Th1 cell lines. *J Immunol* (2008) 180(12):8066–72. doi: 10.4049/jimmunol.180.12.8066

58. Krasemann S, Madore C, Cialic R, Baufeld C, Calcagno N, El Fatimy R, et al. The Trem2-apoe pathway drives the transcriptional phenotype of dysfunctional microglia in neurodegenerative diseases. *Immunity* (2017) 47(3):566–81 e9. doi: 10.1016/j.immuni.2017.08.008

59. Ebner F, Brandt C, Thiele P, Richter D, Schliesser U, Siffrin V, et al. Microglial activation milieu controls regulatory T cell responses. *J Immunol* (2013) 191(11):5594–602. doi: 10.4049/jimmunol.1203331

60. Tripathi P, Tripathi P, Kashyap L, Singh V. The role of nitric oxide in inflammatory reactions. *FEMS Immunol Med Microbiol* (2007) 51(3):443–52. doi: 10.1111/j.1574-695X.2007.00329.x

61. Ham JE, Oh EK, Kim DH, Choi SH. Differential expression profiles and roles of inducible dusps and Erk1/2-specific constitutive Dusp6 and Dusp7 in microglia. *Biochem Biophys Res Commun* (2015) 467(2):254–60. doi: 10.1016/j.bbrc.2015.09.180

62. Habibian JS, Jefic M, Bagchi RA, Lane RH, McKnight RA, McKinsey TA, et al. Dusp5 functions as a feedback regulator of tnfalpha-induced Erk1/2 dephosphorylation and inflammatory gene expression in adipocytes. *Sci Rep* (2017) 7(1):12879. doi: 10.1038/s41598-017-12861-y

63. Sarrazy V, Sore S, Viaud M, Rignol G, Westerterp M, Ceppo F, et al. Maintenance of macrophage redox status by chrebp limits inflammation and apoptosis and protects against advanced atherosclerotic lesion formation. *Cell Rep* (2015) 13(1):132–44. doi: 10.1016/j.celrep.2015.08.068

64. Manoharan I, Hong Y, Suryawanshi A, Angus-Hill ML, Sun Z, Mellor AL, et al. Tlr2-dependent activation of beta-catenin pathway in dendritic cells induces regulatory responses and attenuates autoimmune inflammation. *J Immunol* (2014) 193(8):4203–13. doi: 10.4049/jimmunol.1400614

65. Suryawanshi A, Manoharan I, Hong Y, Swafford D, Majumdar T, Taketo MM, et al. Canonical wnt signaling in dendritic cells regulates Th1/Th17 responses and suppresses autoimmune neuroinflammation. *J Immunol* (2015) 194(7):3295–304. doi: 10.4049/jimmunol.1402691

66. Kuhn SA, van Landeghem FK, Zacharias R, Farber K, Rappert A, Pavlovic S, et al. Microglia express Gaba(B) receptors to modulate interleukin release. *Mol Cell Neurosci* (2004) 25(2):312–22. doi: 10.1016/j.mcn.2003.10.023

67. Crowley T, Cryan JF, Downer EJ, O'Leary OF. Inhibiting neuroinflammation: the role and therapeutic potential of gaba in neuro-immune interactions. *Brain behavior Immun* (2016) 54:260–77. doi: 10.1016/j.bbi.2016.02.001

68. Mayo L, Jacob-Hirsch J, Amariglio N, Rechavi G, Moutin MJ, Lund FE, et al. Dual role of cd38 in microglial activation and activation-induced cell death. *J Immunol* (2008) 181(1):92–103. doi: 10.4049/jimmunol.181.1.92

69. Wang YM, Liu ZY, Ai YH, Zhang LN, Zou Y, Peng QY. Blocking the Cd38/Cadpr pathway plays a double-edged role in lps stimulated microglia. *Neuroscience* (2017) 361:34–42. doi: 10.1016/j.neuroscience.2017.08.010

70. Bahri R, Bollinger A, Bollinger T, Orinska Z, Bulfone-Paus S. Ectonucleotidase Cd38 demarcates regulatory, memory-like Cd8+ T cells with ifn-Gamma-Mediated suppressor activities. *PloS One* (2012) 7(9):e45234. doi: 10.1371/journal.pone.0045234

71. Herrmann MM, Barth S, Greve B, Schumann KM, Bartels A, Weissert R. Identification of gene expression patterns crucially involved in experimental autoimmune encephalomyelitis and multiple sclerosis. *Dis Models Mech* (2016) 9 (10):1211–20. doi: 10.1242/dmm.025536

72. Hu X, Holers VM, Thurman JM, Schoeb TR, Ramos TN, Barnum SR. Therapeutic inhibition of the alternative complement pathway attenuates chronic eae. *Mol Immunol* (2013) 54(3-4):302–8. doi: 10.1016/j.molimm.2012.12.018

73. Jablonski KA, Amici SA, Webb LM, Ruiz-Rosado Jde D, Popovich PG, Partida-Sanchez S, et al. Novel markers to delineate murine M1 and M2 macrophages. *PloS One* (2015) 10(12):e0145342. doi: 10.1371/journal.pone.0145342

74. Sierra-Filardi E, Puig-Kroger A, Blanco FJ, Nieto C, Bragado R, Palomero MI, et al. Activin a skews macrophage polarization by promoting a proinflammatory phenotype and inhibiting the acquisition of anti-inflammatory macrophage markers. *Blood* (2011) 117(19):5092–101. doi: 10.1182/blood-2010-09-306993

75. Niemi K, Teirila L, Lappalainen J, Rajamaki K, Baumann MH, Oorni K, et al. Serum amyloid a activates the Nlrp3 inflammasome *Via* P2x7 receptor and a cathepsin b-sensitive pathway. *J Immunol* (2011) 186(11):6119–28. doi: 10.4049/jimmunol.1002843

76. Madeddu S, Woods TA, Mukherjee P, Sturdevant D, Butchi NB, Peterson KE. Identification of glial activation markers by comparison of transcriptome changes between astrocytes and microglia following innate immune stimulation. *PloS One* (2015) 10(7):e0127336. doi: 10.1371/journal.pone.0127336

77. Boutej H, Rahimian R, Thammisetty SS, Beland LC, Lalancette-Hebert M, Kriz J. Diverging mrna and protein networks in activated microglia reveal Srsf3 suppresses translation of highly upregulated innate immune transcripts. *Cell Rep* (2017) 21 (11):3220–33. doi: 10.1016/j.celrep.2017.11.058

78. Sans-Fons MG, Yeramian A, Pereira-Lopes S, Santamaria-Babi LF, Modolell M, Lloberas J, et al. Arginine transport is impaired in C57bl/6 mouse macrophages as a result of a deletion in the promoter of Slc7a2 (Cat2), and susceptibility to leishmania infection is reduced. *J Infect Dis* (2013) 207(11):1684–93. doi: 10.1093/infdis/jit084

79. Rouillard AD, Gundersen GW, Fernandez NF, Wang Z, Monteiro CD, McDermott MG, et al. The harmonizome: a collection of processed datasets gathered to serve and mine knowledge about genes and proteins. *Database (Oxford)* (2016) 2016. doi: 10.1093/database/baw100

80. Butovsky O, Talpalar AE, Ben-Yaakov K, Schwartz M. Activation of microglia by aggregated β-amyloid or lipopolysaccharide impairs mhc-ii expression and renders them cytotoxic whereas ifn-Γ and il-4 render them protective. *Mol Cell Neurosci* (2005) 29(3):381–93. doi: 10.1016/j.mcn.2005.03.005

81. Butovsky O, Ziv Y, Schwartz A, Landa G, Talpalar AE, Pluchino S, et al. Microglia activated by il-4 or ifn-Γ differentially induce neurogenesis and oligodendrogenesis from adult Stem/Progenitor cells. *Mol Cell Neurosci* (2006) 31 (1):149–60. doi: 10.1016/j.mcn.2005.10.006

82. Shaked I, Tchoresh D, Gersner R, Meiri G, Mordechai S, Xiao X, et al. Protective autoimmunity: interferon-Γ enables microglia to remove glutamate without evoking inflammatory mediators. *J Neurochemistry* (2005) 92(5):997–1009. doi: 10.1111/j.1471-4159.2004.02954.x

83. Butovsky O, Landa G, Kunis G, Ziv Y, Avidan H, Greenberg N, et al. Induction and blockage of oligodendrogenesis by differently activated microglia in an animal model of multiple sclerosis. *J Clin Invest* (2006) 116(4):905–15. doi: 10.1172/JCI26836

84. Ding X, Yan Y, Li X, Li K, Ciric B, Yang J, et al. Silencing ifn-Γ Binding/Signaling in astrocytes versus microglia leads to opposite effects on central nervous system autoimmunity. *J Immunol* (2015) 194(9):4251–64. doi: 10.4049/jimmunol.1303321

85. Willenborg DO, Fordham SA, Staykova MA, Ramshaw IA, Cowden WB. Ifn-gamma is critical to the control of murine autoimmune encephalomyelitis and regulates both in the periphery and in the target tissue: a possible role for nitric oxide. *J Immunol* (1999) 163(10):5278–86. doi: 10.4049/jimmunol.163.10.5278

86. Pierson E, Simmons SB, Castelli L, Goverman JM. Mechanisms regulating regional localization of inflammation during cns autoimmunity. *Immunol Rev* (2012) 248(1):205–15. doi: 10.1111/j.1600-065X.2012.01126.x

87. Haimon Z, Frumer GR, Kim J-S, Trzebanski S, Haffner-Krausz R, Ben-Dor S, et al. Cognate microglia–T cell interactions shape the functional regulatory T cell pool in experimental autoimmune encephalomyelitis pathology. *Nat Immunol* (2022) 23 (12):1749–62. doi: 10.1038/s41590-022-01360-6

88. White MPJ, Webster G, Leonard F, La Flamme AC. Innate ifn-gamma ameliorates experimental autoimmune encephalomyelitis and promotes myeloid expansion and pdl-1 expression. *Sci Rep* (2018) 8(1):259. doi: 10.1038/s41598-017-18543-z

89. Wang Z, Hong J, Sun W, Xu G, Li N, Chen X, et al. Role of ifn-gamma in induction of Foxp3 and conversion of Cd4+ Cd25- T cells to Cd4+ tregs. *J Clin Invest* (2006) 116(9):2434–41. doi: 10.1172/jci25826

90. Venken K, Hellings N, Liblau R, Stinissen P. Disturbed regulatory T cell homeostasis in multiple sclerosis. *Trends Mol Med* (2010) 16(2):58–68. doi: 10.1016/j.molmed.2009.12.003

91. Liu R, Du S, Zhao L, Jain S, Sahay K, Rizvanov A, et al. Autoreactive lymphocytes in multiple sclerosis: pathogenesis and treatment target. *Front Immunol* (2022) 13:996469. doi: 10.3389/fimmu.2022.996469

92. Kwilasz AJ, Grace PM, Serbedzija P, Maier SF, Watkins LR. The therapeutic potential of interleukin-10 in neuroimmune diseases. *Neuropharmacology* (2015) 96(Pt A):55–69. doi: 10.1016/j.neuropharm.2014.10.020

93. Beebe AM, Cua DJ, de Waal Malefyt R. The role of interleukin-10 in autoimmune disease: systemic lupus erythematosus (Sle) and multiple sclerosis (Ms). *Cytokine Growth Factor Rev* (2002) 13(4-5):403–12. doi: 10.1016/s1359-6101(02)00025-4

94. Weber MS, Prod'homme T, Youssef S, Dunn SE, Steinman L, Zamvil SS. Neither T-helper type 2 nor Foxp3+Regulatory T cells are necessary for therapeutic benefit of atorvastatin in treatment of central nervous system autoimmunity. *J Neuroinflamm* (2014) 11(1):29. doi: 10.1186/1742-2094-11-29

95. Jayaraman A, Soni A, Prabhakar BS, Holterman M, Jayaraman S. The epigenetic drug trichostatin a ameliorates experimental autoimmune encephalomyelitis *Via* T cell tolerance induction and impaired influx of T cells into the spinal cord. *Neurobiol Dis* (2017) 108:1–12. doi: 10.1016/j.nbd.2017.07.015

96. Danikowski KM, Jayaraman S, Prabhakar BS. Regulatory T cells in multiple sclerosis and myasthenia gravis. *J Neuroinflamm* (2017) 14(1):117. doi: 10.1186/s12974-017-0892-8

97. Korn T, Reddy J, Gao W, Bettelli E, Awasthi A, Petersen TR, et al. Myelin-specific regulatory T cells accumulate in the cns but fail to control autoimmune inflammation. *Nat Med* (2007) 13(4):423–31. doi: 10.1038/nm1564

98. Korn T, Mitsdoerffer M, Croxford AL, Awasthi A, Dardalhon VA, Galileos G, et al. Il-6 controls Th17 immunity in vivo by inhibiting the conversion of conventional T cells into Foxp3+ regulatory T cells. *Proc Natl Acad Sci United States America* (2008) 105(47):18460–5. doi: 10.1073/pnas.0809850105

99. Koutrolos M, Berer K, Kawakami N, Wekerle H, Krishnamoorthy G. Treg cells mediate recovery from eae by controlling effector T cell proliferation and motility in the cns. *Acta Neuropathologica Commun* (2014) 2(1):163. doi: 10.1186/s40478-014-0163-1

100. Li R, Li H, Yang X, Hu H, Liu P, Liu H. Crosstalk between dendritic cells and regulatory T cells: protective effect and therapeutic potential in multiple sclerosis. *Front Immunol* (2022) 13:970508. doi: 10.3389/fimmu.2022.970508

101. Boddeke EW, Meigel I, Frentzel S, Biber K, Renn LQ, Gebicke-Harter P. Functional expression of the fractalkine (Cx3c) receptor and its regulation by lipopolysaccharide in rat microglia. *Eur J Pharmacol* (1999) 374(2):309–13. doi: 10.1016/S0014-2999(99)00307-6

102. Leonardi-Essmann F, Emig M, Kitamura Y, Spanagel R, Gebicke-Haerter PJ. Fractalkine-upregulated milk-fat globule egf factor-8 protein in cultured rat microglia. *J neuroimmunology* (2005) 160(1-2):92–101. doi: 10.1016/j.jneuroim.2004.11.012

103. Ibáñez-Vega J, Vilchez C, Jimenez K, Guevara C, Burgos PI, Naves R. Cellular and molecular regulation of the programmed death-1/Programmed death ligand system and its role in multiple sclerosis and other autoimmune diseases. *J Autoimmun* (2021) 123:102702. doi: 10.1016/j.jaut.2021.102702

104. Tierney JB, Kharkrang M, La Flamme AC. Type ii-activated macrophages suppress the development of experimental autoimmune encephalomyelitis. *Immunol Cell Biol* (2009) 87(3):235–40. doi: 10.1038/icb.2008.99

105. Brandl C, Ortler S, Herrmann T, Cardell S, Lutz MB, Wiendl H. B7-H1-Deficiency enhances the potential of tolerogenic dendritic cells by activating Cd1d-restricted type ii nkt cells. *PloS One* (2010) 5(5):e10800. doi: 10.1371/journal.pone.0010800

106. Vainchtein ID, Alsema AM, Dubbelaar ML, Grit C, Vinet J, van Weering HRJ, et al. Characterizing microglial gene expression in a model of secondary progressive multiple sclerosis. *Glia* (2023) 71(3):588–601. doi: 10.1002/glia.24297

107. Masuda T, Sankowski R, Staszewski O, Böttcher C, Amann L, Sagar, et al. Spatial and temporal heterogeneity of mouse and human microglia at single-cell resolution. *Nature* (2019) 566(7744):388–92. doi: 10.1038/s41586-019-0924-x

108. Mathys H, Adaikkan C, Gao F, Young JZ, Manet E, Hemberg M, et al. Temporal tracking of microglia activation in neurodegeneration at single-cell resolution. *Cell Rep* (2017) 21(2):366–80. doi: 10.1016/j.celrep.2017.09.039

109. Zocchi E, Daga A, Usai C, Franco L, Guida L, Bruzzone S, et al. Expression of Cd38 increases intracellular calcium concentration and reduces doubling time in hela and 3t3 cells. *J Biol Chem* (1998) 273(14):8017–24. doi: 10.1074/jbc.273.14.8017

110. Subramani J, Ghosh M, Rahman MM, Caromile LA, Gerber C, Rezaul K, et al. Tyrosine phosphorylation of Cd13 regulates inflammatory cell-cell adhesion and monocyte trafficking. *J Immunol* (2013) 191(7):3905–12. doi: 10.4049/jimmunol.1301348

111. Reinhold D, Bank U, Entz D, Goihl A, Stoye D, Wrenger S, et al. Petir-001, a dual inhibitor of dipeptidyl peptidase iv (Dp iv) and aminopeptidase n (Apn), ameliorates experimental autoimmune encephalomyelitis in Sjl/J mice. *Biol Chem* (2011) 392(3):233–7. doi: 10.1515/BC.2011.024

112. Olah M, Amor S, Brouwer N, Vinet J, Eggen B, Biber K, et al. Identification of a microglia phenotype supportive of remyelination. *Glia* (2012) 60(2):306–21. doi: 10.1002/glia.21266

113. Loving BA, Bruce KD. Lipid and lipoprotein metabolism in microglia. *Front Physiol* (2020) 11:393. doi: 10.3389/fphys.2020.00393

114. Kwiatkowski AJ, Helm EY, Stewart JM, Drashansky TT, Cho JJ, Avram D, et al. Treatment with an antigen-specific dual microparticle system reverses advanced multiple sclerosis in mice. *Proc Natl Acad Sci United States America* (2022) 119(43): e2205417119. doi: 10.1073/pnas.2205417119

115. Yang Z, Ming XF. Functions of arginase isoforms in macrophage inflammatory responses: impact on cardiovascular diseases and metabolic disorders. *Front Immunol* (2014) 5:533. doi: 10.3389/fimmu.2014.00533

116. Rath M, Müller I, Kropf P, Closs EI, Munder M. Metabolism *Via* arginase or nitric oxide synthase: two competing arginine pathways in macrophages. *Front Immunol* (2014) 5:532. doi: 10.3389/fimmu.2014.00532

117. Butovsky O, Jedrychowski MP, Moore CS, Cialic R, Lanser AJ, Gabriely G, et al. Identification of a unique Tgf-β–dependent molecular and functional signature in microglia. *Nat Neurosci* (2014) 17(1):131–43. doi: 10.1038/nn.3599

118. Kwidzinski E, Bunse J, Aktas O, Richter D, Mutlu L, Zipp F, et al. Indolamine 2,3-dioxygenase is expressed in the cns and down-regulates autoimmune inflammation. *FASEB J* (2005) 19(10):1347–9. doi: 10.1096/fj.04-3228fje

119. Platten M, Ho PP, Youssef S, Fontoura P, Garren H, Hur EM, et al. Treatment of autoimmune neuroinflammation with a synthetic tryptophan metabolite. *Science* (2005) 310(5749):850–5. doi: 10.1126/science.1117634

120. Yadav MC, Burudi EM, Alirezaei M, Flynn CC, Watry DD, Lanigan CM, et al. Ifn-Gamma-Induced ido and wrs expression in microglia is differentially regulated by il-4. *Glia* (2007) 55(13):1385–96. doi: 10.1002/glia.20544

121. Grohmann U, Fallarino F, Bianchi R, Orabona C, Vacca C, Fioretti MC, et al. A defect in tryptophan catabolism impairs tolerance in nonobese diabetic mice. *J Exp Med* (2003) 198(1):153–60. doi: 10.1084/jem.20030633